





**Master Thesis** 

# Osteopontin - a potential Modulator of Subtype **Identity in Pancreatic Cancer**

By

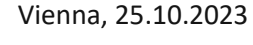
Jonathan Till Abele

Carried out at **Department of General Surgery** Medical University Vienna

Supervision

Supervisor at the Medical University Vienna: Dr. Carl-Stephan Leonhardt

Supervisor at the Technische Universität Wien: Prof. Dr. Robert Mach



## Abstract

Pancreatic ductal adenocarcinoma (PDAC) represents one of the most lethal malignancies worldwide. It is characterized by late diagnosis, limited treatment options and poor prognosis. RNA-sequencing studies revealed two transcriptional subtypes: the classical and the basal-like subtypes. The classical subtype is characterized by epithelial features and high GATA6 expression, whereas the basal-like subtype is associated with an epithelial-mesenchymal transition (EMT) and a poorer histological differentiation.

Patient outcome is correlated with the subtype classification, with the basal-like subtype showing worse overall survival and a faster disease progression. However, this knowledge cannot be exploited for personalized therapeutic approaches since the key drivers of subtype modulation remain unknown. Recently the transcription factor GLI2 and its downstream effector osteopontin (OPN) have been described to modulate subtype identity. The GLI2-OPN circuit can induce and maintain a basal-like cell state 1.

OPN itself is a highly versatile protein that acts in various biological systems. In addition to its role in bone development and in shaping of the immune response, OPN is increasingly implicated with cancer progression. The protein is involved in the induction of an epithelial to mesenchymal transition in tumor cells. Current knowledge assumes, that OPN can interact with several EMT pathways and can activate the tumor microenvironment. These interactions which have been described in multiples tumors, make OPN a potential modulator of subtype identity in PDAC. However, knowledge of its effects in PDAC is very limited and based mostly on results from cancer cell lines <sup>1–3</sup>.

In this thesis I aim to investigate a potential subtype switch upon OPN modulation using a model of patient-derived pancreatic cancer organoids. Additionally, I am to elucidate the involved mechanisms. Organoids retain the transcriptional and genomic heterogeneity of PDAC and are therefore a very wellsuited model to explore the effects of OPN <sup>4</sup>. To analyze the effect of OPN on classical organoids, I treated two classical organoid lines with recombinant OPN, which led to an upregulation of basal-like markers. In addition, treatment of a classical organoid line with conditioned medium from a basal-like organoid line showed a similar effect, indicating the subtype alternating effects of cytokines secreted by basal-like tumor cells. I further wanted to explore whether knocking out OPN would reduce the basal-like signature in a basal-like organoid line. Therefore, I performed a CRISPR/Cas9 mediated OPN ablation in a basal-like organoid line, which led to a strong increase of classical subtype markers, suggesting that OPN is necessary to maintain a basal-like state. However, in a chemotherapeutic drug test, the OPN ablation did not affect the response to standard chemotherapy significantly. Therefore, OPN seems to play a relevant role in the subtype modulation; however, potential effects on chemotherapeutic resistance might be dependent on additional factors, including the tumor microenvironment which is lacking in this *in-vitro* model.

In summary, the present work provides evidence of a subtype-modulating role of OPN in a patient derived organoid model and nominates OPN as a previously unrecognized potential target in the treatment of PDAC.

## **Kurzfassung**

Das duktale Adenokarzinom des Pankreas (PDAC) ist eine der tödlichsten malignen Erkrankungen weltweit, welches sich durch eine späte Diagnose, begrenzte Behandlungsmöglichkeiten und somit einer schlechten Prognose auszeichnet. Mittels RNA-Sequenzierung können zwei transkriptionellen Subtypen unterschieden werden: der klassische Subtyp (classical subtype) und der basale Subtyp ( basal-like subtype). Der classical Subtyp zeichnet sich durch einen epithelien Phänotyp und eine hohe GATA6-Expression aus, während der basal-like Subtyp mit einer epithelial-mesenchymalen Transition und einer niedrigeren histologischen Differenzierung assoziiert ist. Die Klassifizierung des Subtyps erweist sich als klinisch bedeutsam, da der basal-like Subtyp ein schlechteres Gesamtüberleben und ein schnelleres Fortschreiten der Krankheit aufweist. Dieses Wissen kann jedoch nicht in der personalisierten Medizin genutzt werden, da die entscheidenden Wechselwirkungen für das Wechseln des Subtyps noch unbekannt sind. Kürzlich wurde mittels Zelllinien und Xenografte beschrieben, dass der Transkriptionsfaktor GLI2 und sein nachgeschalteter Effektor Osteopontin (OPN) die Subtypausprägung beeinflussen. In diesem Modell kann der GLI2-OPN einen basal-like Zustand induzieren und aufrechterhalten 1.

OPN selbst ist ein äußerst vielseitiges Protein, das in verschiedenen biologischen Systemen wirkt. Neben seiner Rolle bei der Knochenentwicklung oder bei der Initiierung der Immunantwort wird OPN zunehmend mit dem Fortschreiten von Krebserkrankungen in Verbindung gebracht. Es ist weiterhin an der Induktion der epithelialen-mesenchymalen Transition beteiligt, vermutlich durch Interaktion mit verschiedenen EMT-Signalwegen und durch die Aktivierung der Tumormikroumgebung. Diese Wechselwirkungen, die bei einer Vielzahl von Tumoren beschrieben wurden, machen OPN zu einem potenziellen Modulator der Subtyp-Identität bei PDAC. Das Wissen über seine Wirkung bei PDAC ist jedoch sehr begrenzt und basiert vor allem auf Experimenten in Zelllinien 1-3.

In dieser Arbeit versuche ich ein besseres Verständnis vom Einfluss von OPN auf den Tumor Subtyp in PDAC zu bekommen. Hierzu nutze ich ein humanes Organoidmodell des Pankreaskarzinoms, welches aus Tumorproben von Patienten etabliert wurde. Organoide repräsentieren den Tumor deutlich besser als eine klonale Ziellinie, insbesondere durch die Beibehaltung der genomischen und transkriptionellen Heterogenität <sup>4</sup>. Um die Wirkung von OPN auf classical Organoide zu analysieren, habe ich zwei classical Organoid Linien mit rekombinantem OPN behandelt. Eine anschließende Analyse zeigte eine Hochregulierung von basal-like Markern. Darüber hinaus zeigte die Behandlung einer klassischen Organoid Linie mit konditioniertem Medium einer basal-ähnlichen Organoid Linie einen ähnlichen Effekt. Damit konnte gezeigt werden, dass basal-like Organoide Subtyp alternierende Zytokine ausschütten. Die andere Forschungsfrage war, ob ein OPN Knock-Out (KO) die basal-like Signatur in einer basal-like Organoid Linie reduzieren würde. Daher führte ich mittels CRISPR/Cas9 eine OPN-Ablation in einer basal-like Organoid Linie durch. Hier konnte ich einen starken Anstieg der Marker des classical Subtyps nachweisen, was darauf hindeutet, dass OPN für die Aufrechterhaltung eines basallike Zustands notwendig ist. Eine Testung auf Resistenz gegenüber Chemotherapeutika zeigte jedoch keinen signifikanten Unterschied zwischen dem OPN KO und der Wildtyp-Linie. OPN scheint also eine wichtige Rolle bei der Modulation des Subtyps zu spielen, jedoch mögen weitere Faktoren einen möglichen Effekt auf die Chemotherapiesensitivität beeinflussen, u.a. das Tumormikromilieu.

Zusammenfassend zeigt diese Arbeit die wichtige Rolle von OPN für den Erhalt eines basal-like Subtypen auf und liefert weitere Gründe für die Annahme, dass OPN ein mögliches Wirkstoffziel für die Behandlung von PDAC sein könnte.

## Acknowledgments

My great thanks go to Prof. Oliver Strobel, in whose research group I was able to carry out my master's thesis.

Additionally I want to thank Prof. Mach for supervising me at TU Wien, his patience throughout the entire research process and his guidance through my master thesis.

I would like to express my deepest gratitude to my supervisor at Medical University Vienna, Dr. Carl Stephan Leonhardt for his invaluable guidance, mentorship and patience throughout the entire research process. His expertise and insightful feedback were instrumental in shaping this thesis.

Furthermore, I would like to thank Dr. Solange Le Blanc for her support and supervision in the laboratory, her expertise in the organoid culture was essential for executing experiments.

In particular, I would like to thank Dr. Dietmar Pils for his support in the field of bioinformatics, without him the analysis of the scRNA-seq would not have been possible. I also want to thank him for the many stimulating scientific discussions and inspirations.

I am grateful to my colleagues of the research teams of Viszeralchirurgie at AKH Wien for their discussions and shared passion for academic inquiry.

I also want to express my gratitude to my friends and family for their constant encouragement and support during this academic journey.

Special thanks to Katharina Bonitz for her suggestions, encouragement and motivation, which significantly enriched my work.

# Content

ADSITACL	∠
Kurzfassung	3
Acknowledgments	4
1. Introduction	8
1.1 Pancreatic ductal adenocarcinoma	8
1.2 PDAC can be classified into transcriptional subtypes	8
1.3 Osteopontin - a potential subtype modulator of pancreatic cancer	9
1.4 Osteopontin - a potent multifunctional protein	10
1.5 Tumor organoids in cancer research	11
1.6 Aims	12
2. Materials and Methods	13
2.1 PDAC organoids origin and maintenance	13
Origin	13
Organoid medium	13
Organoid thawing	13
Organoid culture and passaging	14
Organoid freezing and storage	14
Mycoplasma testing	14
2.2 Generation of a SPP1 KO organoid line using CRIPSR/Cas9	15
Electroporation	15
Creation of a clonal KO line using single cell selection	15
KO analysis on the DNA level	16
2.3 Drug screening	17
2.4 Treatment of classical organoid lines with recombinant OPN	17
2.5 Treatment of classical organoid lines with conditioned medium from basal-like of	organoids 18
2.6 Analysis of OPN treatment in classical organoids using scRNA-seq	18
Single-cell dissociation and sequencing	18
Single-cell data normalization and analysis	19
2.7 Analysis of the effect of the medium composition on the subtype	19
2.8 Analysis of the intracellular protein content	20

	Immunofluorescence	20
	Protein extraction	20
	BCA Assay	20
	Western Blot	20
	Antibody list	21
	2.9 Analysis of the extracellular protein content	21
	ELISA	21
	Cytokine Array	22
	2.10 Analysis of gene expression	22
	RNA extraction	22
	qPCR	23
	List of Oligonucleotides	24
	2.11 Plasmid constructs	24
	2.12 Statistical analysis	25
3.	. Results	26
	3.1 Selecting appropriate PDAC organoid lines based on subtype identity	26
	3.2 Verification of the RNA sequencing results	27
	Analysis on the RNA level	27
	Analysis at the protein level	28
	Secretome analysis in classical versus basal-like organoids	29
	3.3 CRISPR/Cas9 mediated SPP1 Knock Out in PDO42	30
	Establishment of a SPP1 KO organoid line	30
	An SPP1 KO in a basal-like organoid line shows an effect on subtype markers	32
	An SPP1 KO is not associated with chemotherapy resistance in vitro	33
	3.4 Treatment of classical organoids with recombinant OPN	33
	Exogenous OPN induces a shift of subtype markers in classical organoids	34
	Investigation of subtype markers using single cell RNA sequencing upon treatment recombinant OPN in a classical organoid line	
	Pathway analysis of pseudo bulk scRNA-seq data	37
	3.5 Effects on media composition on PDAC subtype in organoid cultures	39
4	. Discussion	40
•	4.1 Analysis of the organoid cohort	
	Validation of previous characterizations of the organoid cohort	
	Analysis of secreted cytokines	
	- 1	

	4.2 OPN ablation in a basal-like organoid upregulates classical subtype markers	40
	Subtype modulation	40
	An SPP1 Ko does not affect Chemotherapy resistance	41
	4.3 Treatment of classical organoids with OPN	41
	4.4 Conditioned medium from a basal-like organoid line can modify the subtype in a class organoid line	
	4.5 The composition of the culture medium has an influence on the subtype markers	43
	4.6 Limitations	43
	4.7 Conclusion	43
R	References	44

## 1. Introduction

#### 1.1 Pancreatic ductal adenocarcinoma

Pancreatic ducal adenocarcinoma (PDAC), the most common type of pancreatic cancer <sup>5</sup> is estimated to become the second leading cause of cancer related mortality by 2030 6. Despite great efforts and relevant improvements, the 5-year survival rate remains at a modest 11% 7. Due to late diagnosis, only a small portion of patients present with a resectable disease. However, surgical resection is the only chance for cure, usually followed by adjuvant chemotherapy <sup>8,9</sup>. The most common chemotherapy regimens consist of gemcitabine and capecitabine or FOLFIRINOX (folinic acid, 5-flourouracil, irinotecan and oxaliplatin) 10.

## 1.2 PDAC can be classified into transcriptional subtypes

In the past years, genomic studies have revealed the major genetic alteration of the disease and provided a better understanding of the biology behind it. PDAC is usually driven by an activating mutation in KRAS and further mutations of TP53, CDKN2A and SMAD4 11. The KRAS alteration usually affects codon 12, mainly creating a G12D or G12V mutation <sup>12</sup>. In addition to the initial KRAS mutation, the modulation of β-catenin signaling and the expression of Hedgehog ligand allow for PDAC initiation and progression 13.

Based on bulk RNA-sequencing (RNA-seq) studies of the PDAC transcriptome, several subtypes have been described <sup>12</sup>. The most widely used classification distinguishes two subtypes: a classical and a basal-like subtype 12,14-16. The classical subtype is characterized by a higher level of epithelial genes, including the transcription factor GATA6. It is known for its inhibition of dedifferentiation and its suppression of the epithelial to mesenchymal transition (EMT) <sup>17</sup>. The basal-like subtype on the other hand is characterized by the expression of EMT genes, a poor histological differentiation and a worse prognosis 15. Important expression markers associated with the basal-like subtype are GLI2 and ΔNTP63 <sup>1,18</sup>. Both have been described to induce EMT and the switching to a basal-like subtype, especially after GATA6 ablation <sup>17,18</sup>. The basal-like subtype shows parallels to the already described basal-like subtype in bladder or breast cancer 19. In addition to transcriptional changes between the two subtypes it has been possible to differentiate the subtypes on the epigenetic level as well. An analysis of histone modifications and DNA methylation of patient derived xenografts using a clustering approach created two fractions, overlapping with the known PDAC subtypes. The subsequent analysis revealed that basal-like tumors show an upregulation of oncogenic pathways such as the Wnt pathway, EMT or the TGFβ pathway. In contrast, the classical subtype featured pathways and genes associated with the pancreatic development, including BMP2, GATA6 or SHH. For the basal-like subtype the MET gene was identified as a strong regulator 20. With the advent of single-cell sequencing technologies it is possible to characterize the transcriptomic subtype for each cell of a whole tumor. With this analysis it was possible to find a subset of tumors with a heterogeneous subtype identity, containing both classical and basal-like cells <sup>21,22</sup>. Additionally, it was shown, that co-expressor cells exist in a majority of tumors. These cells express classical as well as basal-like markers. A spatial analysis showed that these co-expressor cells were a possible transitional phenotype between the classical and basal-like phenotype <sup>23</sup>. Thus, it was assumed, that the subtype identity is plastic and can be modulated. Beside transcriptional changes there are other possible drivers for subtype identity. Firstly, it has been suggested that copy number alteration of mutant KRAS play a major role <sup>22</sup>. Secondly, the cell of origin could play an important role in the PDAC subtype formation. After establishing that acinar and ductal cell-derived tumors are transcriptionally distinct, it was shown that basal-like PDAC is associated with a ductal signature and classical PDAC is associated with an acinar signature <sup>24</sup>. Thirdly, exogenous factors of the tumor microenvironment (TME) are thought to affect the tumor subtype as well <sup>25</sup>.

In addition to the distinct subtypes of the cancer cells, there are descriptions of different subtypes in the tumor stroma as well <sup>15</sup>. The stroma constitutes up to 85 % of the tumor volume, making PDAC one of the most stroma rich solid tumors. The stroma consists of a dense extracellular matrix (ECM) populated with cancer associated fibroblasts (CAF), immune cells, and others. The dense ECM creates a tumor microenvironment with hypoxic conditions and limits the delivery of nutrients or chemotherapeutics to the tumor <sup>26,27</sup>. CAFs constitute the biggest part of the stroma and produce most of the ECM proteins and cytokines. Early studies showed that CAFs can support or restrict tumor growth <sup>28</sup>. With the use of single cell sequencing techniques, CAFs were classified into myofibroblasts (myCAFs) and inflammatory CAFs (iCAFs). Whereas myCAFs are proposed to be tumor restrictive, iCAFs express high levels of inflammatory cytokines and promote tumor progression <sup>29</sup>. The secreted cytokines can promote EMT and proliferation of cancer cells <sup>30,31</sup>. Furthermore, the secretion of nichefactors by CAFs seems to be an important regulator of PDAC subtypes. Especially the classical subtype shows a high niche factor dependency <sup>25</sup>. Unfortunately, it seems possible, that with the ablation of CAFs, tumor cells would de-differentiate into the niche-factor-independent basal-like phenotype <sup>25,32</sup>.

Since the classification of the basal-like and classical subtype, these subtypes have been associated with different clinical prognosis. Especially the basal-like subtype is related to a lower progression free and overall survival of patients. Using the ICGC database basal-like cancer patient showed a median survival time of 11 months compared to 19 months with the classical subtype 15. This considerably worse prognosis of the basal-like subtype is partly attributed to a reduced chemotherapy sensitivity. In a cohort of 12 basal-like patients only one achieved a partial response (PR) with a first line FOLFIRINOX or gemcitabine/nab-paclitaxel therapy. In comparison, 13 from 38 classical patients achieved a PR. In addition to the inferior chemotherapy resistance in-vivo, the basal-like subtype is mostly associated with an initial metastatic disease <sup>33</sup>. In a different study, patient derived organoids (PDOs) with a basal-like subtype would be more likely oxaliplatin non-sensitive. This is especially unfortunate, since the oxaliplatin signature correlates stronger with the FOLFIRINOX response, compared with the 5-FU or SN-38 signature <sup>34</sup>. In the PDO cohort used in this thesis a link between the non-sensitivity to 5-FU and a reduced drug response with the basal-like organoids could be shown <sup>21,35</sup>. Unfortunately, chemotherapy treatment itself can induce a more basal-like and therefore more aggressive disease 22,36,37.

## 1.3 Osteopontin - a potential subtype modulator of pancreatic cancer

One of the described subtype regulators is the transcription factor GLI2. Using the pancreatic cancer cell line YAPC it could be shown that a GLI2 overexpression induces an upregulation of mesenchymal markers and a downregulation of epithelial markers and GATA6. Additionally, GLI2 seems to be required for a basal-like state. In a GLI2 Knock Out (KO) model in KP4 cells, the expression of basal-like markers was significantly reduced and tumor xenografts displayed a reduced growth in-vivo. GLI2 expression could as well be associated as an additional mechanism for tumor growth in case of KRAS ablation. The basal-like subtype has previously been described as resilient to an KRAS inhibition <sup>1,38</sup>.

A further analysis of possible downstream targets of GLI2, that drive the subtype change led to Secreted Phosphoprotein 1 (SPP1). SPP1 was one of the most upregulated transcripts after an induced GLI2 overexpression in the YAPC cell line. SPP1 encodes Osteopontin (OPN) a mostly secreted phosphorylated glycoprotein. An initial SPP1 promoter analysis showed that GLI proteins can bind upstream of the translational start side <sup>39</sup>. Importantly, treatment with recombinant OPN was capable of inducing basal-like genes in the classical PDAC cell line CAPAN2 and could rescue the basal-like expression after a GLI2 ablation. Exogenous OPN seems therefore capable to induce a subtype switch. On the other hand, a SPP1 KO cell line showed an increase of classical markers. A strong indicator for the role of OPN in tumor progression and metastasis was the strong growth inhibition of a SPP1 KO

tumor xenograft. Therefore, the GLI2-OPN axis seems to play a key role in the initiation and maintenance of a basal-like subtype 1.

### 1.4 Osteopontin - a potent multifunctional protein

Osteopontin was named based on its function as a major non-collagenous bone matrix protein <sup>40</sup>. It can account for up to 2 % of the non-collagen bone mass and regulates bone development 41. In this role it affects the migration of mesenchymal stem cells and osteoclasts <sup>42,43</sup>. OPN belongs to the small integrin-binding ligand N-linked glycoprotein (SIBLING) family. The integrin binding domain RGD 44 is highly conserved (Fig. 1 - A) among vertebrates. Additionally further binding domains are present (Fig. 1 - B), most importantly one for CD44 (a PDAC tumor stem cell marker 45) making OPN a multifunctional ligand <sup>46</sup>. Furthermore, multiple post translational modification sites (mainly phosphorylation and glycosylation), different splicing isoforms, proteolytic cleavage sites and crosslinking sites show the versatility of OPN <sup>47</sup>. An OPN variant, lacking the ΔN region with the secretion signal sequence, forms an intracellular OPN form. This form is mostly associated with the regulation of cytoskeletal rearrangement and signal transduction pathways such as Toll-like receptor pathways <sup>48</sup>. The expression of OPN is regulated by TGFβ through SMAD signaling pathways, AP1 or GLI proteins <sup>39,49,50</sup>.

Besides its role in the bone matrix, OPN is secreted by multiple cells from the immune system (including neutrophils, dendritic cells, T cells and B cells) acting as a cytokine. During inflammation, the primary function of OPN involves activating various leukocytes to generate a functional response thereby modulating the overall immune response. Beside stimulating migration, the activated immune cells secret further cytokines promoting the inflammatory response 51.

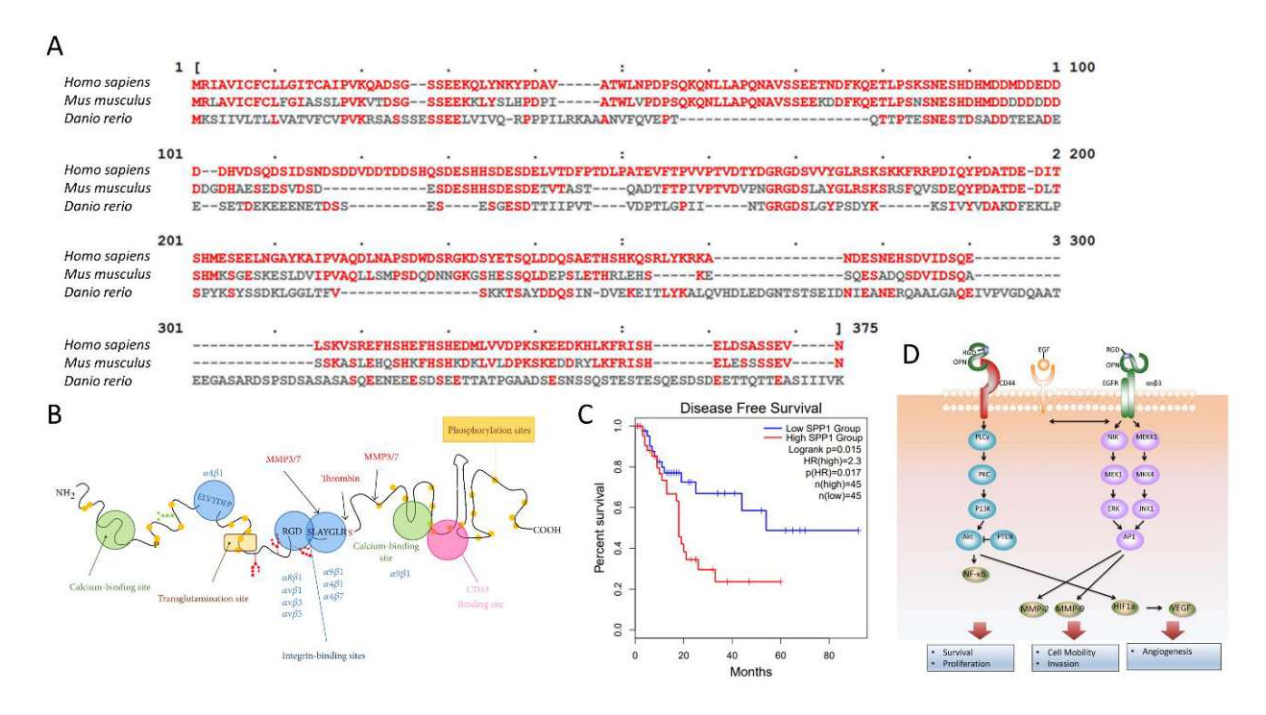


Figure 1: Properties of OPN. A, OPN is a highly conserved protein found in many species. Especially the RGD domain, at 170 AA is conserved among vertebrates. In Homo sapiens it represents the integrin binding domain. B, the main domains of OPN are shown, published by 51. C, survival analysis based on the SPP1 expression (top 25 % in red versus bottom 25 % in blue) 52. D, the pathways of OPN in cancer progession and metastasis are shown, pubslished by.  $^{2}.$ 

Besides its involvement in normal physiological processes, OPN binds to multiple receptors which are associated with signaling pathways involved in cancer. Thus, a high OPN expression can be linked to multiple aggressive malignancies: e.g., breast cancer, prostate cancer and glioblastoma 53. OPN can activate various pathways: NF-kB (via integrins or CD44) - inducing cell survival and proliferation, AP1 (via integrins and EGF utilizing the NIK, ERK or the MEKK1-JNK pathways) - promoting cancer cell

motility. Further downstream targets include HIFa and VEGF, leading to angiogenesis and cancer progression (Fig. 1 - D) <sup>2,54</sup>. In addition to the activation of tumorigenic signaling pathways, OPN is associated with mediating EMT. With the transition towards a mesenchymal phenotype, cancers cells undergo a cytoskeletal reorganization and gain cellular motility, promoting metastasis. It was shown, that many important EMT pathways (such as TWIST, ZEB, SNAIL) show interactions with OPN. However, these findings are from other cancer entities than PDAC 3,55,56. In addition to modulating EMT via regulatory pathways, OPN was described to modify the tumor microenvironment to support EMT. Here, OPN supports the emergence and activation of CAFs <sup>57</sup>. These CAFs secret EMT promoting cytokines, such as IL6 3,58. Therefore, OPN overexpression can be linked to disease progression and metastasis in various cancers 59.

For PDAC itself there are only few reports describing the negative effects of a high OPN expression <sup>51,53,60</sup>. An indication of the negative effects of high OPN levels in PDAC is a survival analysis based on the expression status of the SPP1 gene. In the GEPIA2 52 dataset the highest 25 % of SPP1 expressing tumors showed a strongly decreased progression free survival, compared with the lowest 25 %. The high hazard ration can link SPP1 expression towards an unfortunate prognosis, making OPN in PDAC an interesting target for further research (Fig. 1 - C).

Currently OPN is not druggable, although many studies have shown the efficacy of an OPN inhibition for various diseases in preclinical models <sup>61–63</sup>. One issue in the development of new drugs is the high physiological turnover rate of OPN ( $t_{1/2} \sim 11$  min.) <sup>64</sup>. This might be an explanation for the failure of therapeutic anti-OPN antibodies in the clinical setting 65.

## 1.5 Tumor organoids in cancer research

Currently, a major challenge in cancer research is the translation of observations from the bench to the patient. Unfortunately, many drugs, which show a strong effect in a preclinical cancer models fail to show a benefit in the clinic. One of the reasons is the difficulty of creating reliable models matching the individual patient's tumor. The most commonly used cancer research model are cancer cell lines. Although they have contributed to massive advancements in the understanding of cancer biology, they have several drawbacks. Most importantly, only a few cells in each tumor have the ability to grow for multiple passages under 2D culture conditions <sup>4</sup>. This results in a loss of heterogeneity, since a clonal cell is selected, which has undergone multiple genetic alternations. Furthermore, the 3D structure of the tumor and the surrounding tissue is missing completely. A more complex model are patient derived tumor xenografts (PDTX). In this model tumor tissue is transplanted into immunodeficient mice. The PDTX model can maintain the tumor heterogeneity for multiple passages. Disadvantages are the replacement of human stroma with murine stroma and the enormous costs of maintaining this model 4,66,67

Advantages in stem cell research led to the development of organoids. Using the media conditions identified by this progress a novel 3D in-vitro cancer model was established in the last 10 years, termed cancer organoids <sup>68</sup>. By providing a 3D matrix and growth factors, tumor cells are able to grow, while still resembling genetically and phenotypically the original tumor. The culture medium mimics conditions required for stem cell growth. Since healthy cells can form organoids as well, selective medium (e.g. lacking WNT and R-Spondin1) can be used to create only tumor organoids. Furthermore, the success rate to establish patient derived tumor organoids is higher than 2D models. To model the tumor microenvironment co-cultures approaches have been described <sup>4</sup>. Additionally, organoids can be transplanted into mice creating xenograft in-vivo models. Furthermore, a wide range of experimental techniques is available in organoids, including genetic modifications using the CRISPR/Cas9 system. In particular, organoids can be used for personalized drug testing to identify



individual vulnerabilities <sup>69</sup>. Disadvantages are the higher maintenance efforts and the comparably slow growth 4,69-71.

#### 1.6 Aims

The subtype of a pancreatic cancer patient is an important prognostic factor. However, it is currently not possible to exploit the knowledge about the subtypes for a clinical benefit. The main reasons are the still poorly understood molecular mechanisms regarding subtype modulation. There are multiple genes thought to have an impact on the subtype identity. One of these is OPN. The aim of this thesis was to better elucidate the relationship between OPN and subtype identity in patient-derived pancreatic cancer organoids.

Specifically, two main experiments were conducted. Firstly, the goal was to investigate the effects of exogeneous OPN in classical organoid lines and potential subtype modulations. Furthermore, the effects were to be characterized using single cell RNA-sequencing. The second goal was to investigate the effects of an SPP1 loss in a basal-like organoid line on transcriptomic subtype and chemotherapy resistance.

## 2. Materials and Methods

## 2.1 PDAC organoids origin and maintenance

#### Origin

The pancreatic tumor organoid cultures were established in previous research programs <sup>21,35</sup>. The tumor tissue to develop organoids was extracted from patients admitted at the Department of General, Visceral and Transplantation Surgery, Heidelberg University Hospital. Prior to surgery, all patients had given their informed written consent regarding the acquisition of tissue. The study was approved by the Ethics Committee of Heidelberg University (ethic votes 301/2001, 159/2002, S-206/2011, S-708/2019) 35. The process to establish tumor organoids cultures was an adaption of a protocol previously described in the literature <sup>21,35</sup>.

The organoid cohort was analyzed regarding the representation of the original tumor. It was shown that the organoids can resemble the original tumor heterogeneity on a transcriptional level and can maintain the transcriptional subtypes 35. Additionally, it was possible to use data obtained from organoids for predicting patient outcome. For each organoid a subtype score was created using nonnegative matrix factorization 35.

#### Organoid medium

For maintaining and working with the organoid culture two media compositions were created. The basal organoid media consists of 500 ml of Advance DMEM/F12 medium (Gibco, United States) supplemented with 5 ml of 200 mM Glutamax (Gibco), 5 ml of 1 M HEPES (Gibco) and 1 ml of 500x Primocin (Gibco). The main culture medium was the tumor organoid medium (EFWsRcNA). It consist of basal tumor organoid medium supplemented with 1x B-27 supplement (Gibco), 1 mM Nacetylcysteine (Sigma Aldrich, United States), 50 ng/ml EGF (PeproTech, United Kingdom), 100 ng/ml FGF10 (PeproTech), 0.5 nM Wnt surrogate (ImmunoPrecise, United States), 10 % RSPO1-conditioned medium, 100 ng/ml Noggin (PeproTech), 500 nM A83-01 (TOCRIS, United Kingdom) and if necessary 10 μM Y-27632 (Selleckchem, United States). Both media were prepared on ice and kept in a 4 °C fridge until further use. For the scRNA-seq experiment, it was required to work under serum-free conditions. In these cases, a tumor organoid medium without Wnt surrogate was prepared. Contrary to reports 72 which show a Wnt dependency of a portion of PDAC organoids, the used organoid lines should not be affected by a short Wnt withhold 35. The organoids are seeded in a 3D-matrix. In this case the chosen material was a phenol red free growth-factor reduced Matrigel (Corning). Matrigel is a complex mixture of ECM proteins, mostly laminin, collagen IV and enactin. Matrigel can be extracted from Englebreth-Holm-Swarm tumors in mice 73,74. For handling the Matrigel it was necessary to keep it always on ice and for pipetting to use cold tips, since Matrigel solidifies at higher temperatures than 4 °C.

#### Organoid thawing

For long term storage PDAC patient derived organoids were kept in a liquid nitrogen tank. To start a new culture, the cryovial containing the organoids was thawed in a 37 °C water bath. The organoids were frozen in a mixture of Matrigel and DMSO for cryoprotection. DMSO however has toxic effects at higher temperature and had to be removed quickly. The content of the vial was transferred to a 15 ml falcon containing 9 ml basal organoid medium. The falcon was centrifuged at 4 °C with 300 g for 5 min and the supernatant was carefully removed, leaving a small Matrigel layer. Afterwards the Matrigel layer containing the organoids was resuspended in a similar volume of fresh Matrigel. The organoids were seeded in two 50 µl Matrigel domes per Well of a prewarmed 12-Well CytoOne Plate, TC-treated (Starlab, Germany). The plate was incubated for 15 min in a cell culture incubator to speed up the solidification of the Matrigel. Finally, 1 ml of tumor organoid medium supplemented with 10  $\mu$ M Y-27632 was pipetted into each well. The outer six wells were not used and instead filled with 1 ml of



PBS to reduce evaporation of the cell culture medium. For the duration of the cell culture the organoid culture was kept in a cell culture incubator HERACELL 150i (Thermo Fisher) set to 5 % CO2 and 37 °C. The medium was changed every 3-5 days without the supplemented Y-27632.

#### Organoid culture and passaging

The organoids were passaged depending on growth, but at least every two weeks. Initially the culture medium was removed from each well. The medium was collected at -20 °C for mycoplasma testing. To mechanically dissociate the organoids and to break down the Matrigel dome 1 ml of TrypLE Express (Thermo Fisher) supplemented with 10 μM Y-27632 was pipetted up and down. The resulting suspension was transferred to a 15 ml falcon and incubated at 37 °C in a water bath. After 15 min and repeated pipetting the dissociation was stopped by the addition of 9 ml of cold basal organoid medium. The suspension was centrifuged at 4 °C with 300 g for 5 min. The supernatant was removed without disturbing the cell pellet. The cells were resuspended in 100 µl of basal organoid medium. To determine the cell number 10 µl of the suspension was mixed with 10 µl of a trypan blue solution (Sigma Aldrich, United States). Using the LUNA-FL™ Dual Fluorescence Cell Counter (Logos Biosystems, South Korea), the cells were counted. Depending on the organoid line the seeding density, usually 15.000 – 30.000 cells/50 μl Matrigel, was defined. According to the seeding plan and the cell number, the necessary suspension volume was transferred to a 15 ml falcon. After the addition of 1 ml basal organoid medium, it was centrifuged at 4 °C with 300 g for 5 min. In order to completely remove the supernatant, the pellet was centrifuged again for one minute after discarding the supernatant. When the remaining supernatant was removed, the cell pellet was resuspended in Matrigel. In each well of a prewarmed 12 WP two 50 µl Matrigel domes could be seeded. After incubating the well plate for 15 min in an incubator, 1 ml of tumor organoid medium supplemented with 10 μM Y-27632 was pipetted to each well. The medium was afterwards changed every 3-5 days without the previously supplemented Y-27632.

#### Organoid freezing and storage

To preserve the established organoid lines for further experiments and to have a back-up in case of need, it is essential to keep a frozen organoid stock. To increase the stocks, it is necessary to freeze an organoid surplus away. For a good recovery after thawing, a high number of small organoids should be frozen. The protocol started with a resuspension of the two Matrigel domes in 1 ml tumor organoid medium. The original medium should be kept for mycoplasma testing. The organoid suspension was transferred to a 15 ml falcon filled with 9 ml of basal organoid medium. This was consequently centrifuged at 4 °C with 300 g for 5 min. The supernatant was discarded and the Matrigel layer was resuspended, first in 100 μl, and then in 1 ml of cold Recovery Cell Culture Freezing Medium (Gibco) supplemented with 10  $\mu$ M Y-27632. The suspension was transferred to precooled cryovials. For a slower cooling rate, the cryovials were inserted into a CoolCell freezing container (BioCision, United States) and placed in a -80 °C fridge. After at least 24 h the cryovials were transferred to their final storage location, a liquid nitrogen tank.

#### Mycoplasma testing

All organoid lines were routinely tested for Mollicutes contamination. The Venor®GeM kit (Minerva Biolabs, Germany) was used according to the manufacturer's instructions. The test is based on the specific amplification of the 16S rRNA coding region in bacterial DNA. The test only amplifies DNA from certain Mycoplasma, Acholeplasma and Spiroplasma species. First, 100 μl of cell culture supernatant was transferred to a 1.5 ml tube and incubated at 95 °C for 10 minutes. To remove cellular debris, the sample was centrifuged at maximum speed for 20 s. From this sample, 2 µl were used for the PCR. A mix consisting of 15.3 µl nuclease free water, 2.5 µl 10x reaction buffer, 2.5 µl primer/nucleotide mix, 2.5 µl internal control DNA and 0.2 µl MB Taq polymerase (5U/µl) (Minerva Biolabs) was used for the PCR. 2 µl of sample was added to this mixture. A positive and a negative control were included in each



PCR run. The sample was mixed before it was put on a thermocycler. The PCR settings were: 94 °C for 2 min and afterwards 39 cycles with 94 °C for 30 s, 55 °C for 30 s and 72 °C for 30 s. After a final extension at 72 °C for 30 s, the PCR was finished and the products were separated on an 2 % agarose gel. The gel was run at 100 V for 20 min. The expected amplicons were in the range of 191 bp for the internal control and around 270 bp for Mycoplasma spp.

## 2.2 Generation of a SPP1 KO organoid line using CRIPSR/Cas9 Electroporation

For the expression of the CRISPR/Cas9 system an electroporation-based plasmid delivery system was chosen. For this transfection three different plasmids were used: a pX330 expression vector (Addgene #42230) with a cloned gRNA targeting SPP1 (AGGCATCACCTGTGCCATAC) or for the non-targeting control (GTATTACTGATATTGGTGGG), a Super PiggyBac transposase expression vector (BioCat, Germany) and a PiggyBac Expression vector PB513B-1 containing a Puromycin resistance and a GFP gene (BioCat). To ensure an appropriate number of cells for the transfection, multiple wells from the same organoid line PDO42 were pooled after the last centrifugation step before the cell count. After removing the culture medium, the organoids were mechanically dissociated by pipetting them while resuspending them in a dissociation medium 1 ml of TrypLE Express (Thermo Fisher) per well containing 10  $\mu$ M Y-27632. The medium was transferred to a 15 ml Falcon tube and incubated for 15 minutes at 37 °C with repeated pipetting steps. The dissociation was stopped with the addition of 10 ml of basal medium. To remove the TrypLE Express the suspension was centrifuged at 4 °C with 300 g for 5 min. The following steps, apart from the electroporation were always conducted on ice. Afterwards the cells were resuspended in 100 µl of basal medium and further diluted in additional 3 ml before the cells were strained with a 40 µm cell strainer. Afterwards the cells were centrifuged again and resuspended in 100 μl of Opti-MEM (Thermo Fischer) and counted. For the electroporation 200.000 cells were selected and added to the pre-mixed plasmids. The volume of the suspension was adjusted to 100 µl with additional Opti-MEM. The final plasmid concentration was: 100 µg/ml for pX330, 72 µg/ml for the PiggyBag expression vector and 28 µg/ml for the Super PiggyBag transposase expression vector. The mixture was then transferred to a 2 mm electroporation cuvette and placed in the electroporator NEPA21 (Nepa Gene, Japan). For the electroporation, the following settings were used: 5 pulses with 20 V for 50 ms with an interval of 50 ms while the decay rate was set to 40 %. Immediately afterwards 400  $\mu$ l of basal medium supplemented with 10  $\mu$ M Y-27632 and 5  $\mu$ M CHIR99021 were added and the mixture was incubated for 30 min at room temperature. Afterwards the cells were recovered and centrifuged at 4 °C for 5 min at 300 g. The supernatant was removed and the organoids were resuspended in 50 µl of Matrigel. Afterwards the cells were seeded in two 25 µl domes on a 24 WP. To speed up the solidification of the Matrigel the plate was placed for 10 min in the 37 °C incubator. Afterwards 500 µl of antibiotic free tumor organoid medium supplemented with  $10 \,\mu M$  Y-27632 and  $5 \,\mu M$  CHIR99021 was pipetted in the wells. The cells were placed in a 30 °C incubator for 2 consecutive days. After a week, the organoids success of the transfection was verified using a UV microscope looking for GFP positive cells. When the organoids had recovered, they were selected using tumor organoid medium containing 2 µg/ml Puromycin for 3 days. This puromycin concentration for the organoid line PDO42 was experimentally obtained earlier. Afterwards the organoids could recover in fresh tumor organoids medium. After expanding the new organoid line SPP1 KO bulk and non-targeting control both derived from PDO42 could be characterized and analyzed.

## Creation of a clonal KO line using single cell selection

In order to obtain a clonal knock-out organoid line, a single cell from the SPP1 KO bulk line had to be selected, grown out and afterwards characterized. In this case a serial dilution was chosen to achieve the seeding of multiple single cells per well. After recovery from the puromycin selection and following

expansion, it was possible to passage the organoids for a clonal selection. This started by removing the culture medium and the mechanical dissociation of the organoids by pipetting them in a dissociation medium of 1 ml TrypLE Express supplemented with 10 µM Y-27632. The medium was transferred to a 15 ml Falcon tube and incubated for 15 minutes at 37 °C with repeated pipetting steps. The dissociation was stopped with the addition of 10 ml of basal medium when a proper dissociation could be observed under the microscope. To remove the TrypLE Express the suspension was centrifuged at 4 °C with 500 g for 5 min. From now on, the cells were always kept on ice. Afterwards the cells were resuspended in 100 µl of basal medium and diluted in additional 3 ml before being strained with a 40 μm cell strainer. Afterwards the strained cells were centrifuged again and resuspended in 100 μl of basal organoid medium and counted. For the fluorescence counting 2 µl of Acridine Orange /Propidium lodide staining solution (Logos Biosystems) were mixed with 18 μl of the cell suspension in a 1,5 ml tube. 10 µl of the mixture was loaded into a PhotonSlide™ and the cell viability and number were determined using the LUNA-FL™ Dual Fluorescence Cell Counter. Depending on the cell count, the necessary volume for 600 cells were taken from the cell suspension and transferred to a 15 ml falcon. If small volumes had to be pipetted, the cell suspension was first diluted and then the process of counting was repeated. Subsequently, 1 ml of the basal organoid medium was added to the Falcon, before a final centrifugation step at 4 °C with 300 g for 5 min in order to remove the supernatant. The cells were resuspended in 150 μl of a 50 % Matrigel / tumor organoid medium mixture. Starting with this dilution, a 1:2 dilution series from 20 cells/ 5 µl down to 0.3 cells / 5 µl was established. For this, 75 μl of the respective dilution were mixed with 75 μl of the 50 % Matrigel / tumor organoid medium mixture. Into each well of a prewarmed 96 WP, 5 μl of a dilution were added to form a Matrigel dome. Each row of the WP contains its own dilution. To allow the Matrigel domes to solidify, the WP is placed in the 37° C cell culture incubator for 15 min. Afterwards 100 μl of prewarmed tumor organoid medium supplemented with 10 μM Y-27623 was added to every well. On the same day, every well was analyzed under the microscope for single cells. These wells were marked and further monitored. The medium was exchanged every 3 to 4 days. After formation of the organoids, each was analyzed in a UV microscope for a GFP signal. All GFP+ growing organoids from the marked wells were passaged and seeded in a new 5 µl Matrigel dome. In total, two clonal organoid lines were able to grow. These two were named clone 1 and clone 2, both deriving from the SPP1 KO bulk from PDO 42. They were expanded for further characterization and experiments.

#### KO analysis on the DNA level

In order to analyze the results of the CRISPR/Cas9 mediated *SPP1* KO in the organoid line PDO42 it was necessary to extract genomic DNA. During a passage, excess cells would be used. The cells were added to a 1.5  $\mu$ l tube and centrifuged for 5 min at 300 g. The supernatant was removed, and the cells were resuspended in 200  $\mu$ l of PBS. For extracting the DNA the QlAamp DNA mini kit (Qiagen) was used according to the manufacturer's instructions. The following reagents were included in the kit. Now 20  $\mu$ l of proteinase K and afterwards 200  $\mu$ l of Buffer AL was added to the cell suspension. Before a 10 min incubation at 56 °C, the mixture would be vortexed. Afterwards 200  $\mu$ l of ethanol were added, before further vortexing. The resulting mixture was transferred to a QlAamp Mini spin column and centrifuged at 6,000 g for 1 min. After discarding the flowthrough 500  $\mu$ l of buffer AW1 were added and the column was centrifuged, and the flowthrough was discarded again. In an additional washing step, 500  $\mu$ l of buffer AW2 were added before a 3 min centrifugation step at maximum speed. Finally, the DNA was collected in a fresh 1.5 ml tube by a centrifugation at 6,000 g for 1 min using 50  $\mu$ l of distilled water as an eluent. The DNA was stored at -20 °C before further use.

To amplify the region of interest and make it available for sanger sequencing a PCR was performed. For Analysis of the *SPP1* KO two primers were designed beforehand to cover the potential region of the CRISPR cut: fw TCCCTTTCCCTTGCCTAATAGT and rev TGCACCTCTCGCCATAATTG. For the PCR, the

Q5® High-Fidelity 2X Master Mix (NEB, United States) was used according to the manufacturer's instruction. In a first step the 1  $\mu$ l of the sample DNA, 12.5  $\mu$ l of the master mix, 1.25  $\mu$ l of each 10  $\mu$ M Primer and 9 µl of nuclease free water were mixed in a PCR tube. The sample was mixed before it was put on a thermocycler. The PCR settings were: 98 °C for 30 s and afterwards 25 cycles with 98 °C for 30 s, 66 °C for 30 s and 72 °C for 30 s. After a final extension at 72 °C for 2 min the PCR was finished and the products were separated on an agarose gel. To separate the amplicon with a size of 499 bp an agarose concentration of 1.5 % was chosen. To detect the DNA Gelred (Biotium, United States) was used. The gel was run at 110 V for 70 min. Afterwards the amplicon was cut out, weighted and purified. To purify the PCR product NucleoSpin kit (Macherey-Nagel, Germany) was used according to the manufacturer's instructions. The following reagents were included in the kit. The Gel containing the DNA of interest was dissolved in 200 µl NTI buffer / 100 mg of gel. The suspension was incubated at 50 °C for 10 min until everything was dissolved. To speed up the process, the mixture was regularly vortexed. The suspension was transferred to the NucleoSpin column and centrifuged at 11,000 g for 30 s. After discarding the flowthrough 700 µl of NT3 were added and the mixture was centrifuged again. This step would be repeated to increase the purity of the sample. Afterwards the column was dried with an empty centrifugation step a 11,000 g for 1 min. Finally, the 15 µl of NE buffer was added to the column. After a short incubation, the DNA was eluted with a last centrifugation at 11,000 g for 1 min. The DNA concentration was measured using the NanoDrop. For sequencing the DNA was diluted to 5 ng/µl and sent to Eurofins Genomics for Sanger Sequencing. To analyze the KO efficiency the ICE tool <sup>75</sup> (Synthego, United States) was used.

#### 2.3 Drug screening

To assess the effects of the OPN ablation regarding chemotherapy resistance, drug screening was performed. Three common chemotherapeutic drugs were chosen from the FOLFIRINOX regimen: 5flourouracil (5-FU), oxaliplatin (OXA) and the active component from irinotecan (SN-38). The drug concentrations and treatment durations were chosen based on previous studies.<sup>34,35</sup> The seeding conditions were 1.000 cells / 5 µl growth-factor reduced Matrigel dome (Corning, United States) per well of a 96-well μCLEAR microplate (Greiner, Austria). To ensure that the organoids had similar sizes the organoids were previously strained with a 40 µm cell strainer (Corning, United States). To prevent negative edge effects, the outer wells were not seeded and filled with PBS instead. Each condition was assayed in triplicates. The organoids were exposed to a maximum of 5% DMSO, therefore respective controls were included. For the drug test three different organoid lines were chosen: PDO 42 (wildtype), CRISPR control (derived from PDO 42) and SPP1 KO clone 2 (derived from PDO 42 as well). Initially organoids were grown for three days in 100 µl of tumor organoid medium. Afterwards the medium was replaced with drug containing medium. After additional three days the medium was removed, and the wells were washed two times with basal organoid medium. For further three days the organoids were kept in drug free tumor organoid medium. Finally, the viability was measured using the CellTiter-Glo 3D Cell Viability assay (Promega, United States) according to the manufacturer's instructions. After adding 100 µl of CellTiter-Glo 3D Reagent per well, the plate was placed for 5 minutes on an orbital shaker and was incubated for additional 25 min at room temperature. The chemiluminescence was measured on a microplate reader. GraphPad Prism was used to create a visual and statistical interpretation of the results.

#### 2.4 Treatment of classical organoid lines with recombinant OPN

Since previous reports <sup>1</sup> showed a translational subtype switching of pancreatic cancer cell lines upon OPN treatment, we aimed to reproduce this effect using a patient derived pancreatic cancer organoid model. Because a thorough analysis of this effect was planned using a scRNA-seq approach, the first objective was to find OPN treatment conditions, which show a strong response. For this task two organoid lines expressing a classical signature were chosen: PDO18 and PDO81. Since the PDO18 grew



faster compared to PDO81, the seeding density of PDO81 was increased during the experiment from initially 15.000 cells/50 μl Matrigel to 25.000 cells/50 μl Matrigel. The organoids were grown in serum free tumor organoid medium, without the supplementation of Wnt. For treatments longer than 6 days the organoids were passaged after one week. The treatment consisted of tumor organoid medium supplemented with recombinant human OPN (R&D Systems, United States). The concentration of the supplemented OPN varied between 0.5 and 1 μg/ml. In addition to the treated organoids, in parallel non treated organoids were grown as a control group. For determining the response RNA was isolated at the end of the experiment and a qPCR analysis, comparing the control with the treated organoids, using classical and basal-like marker gene expression was performed.

## 2.5 Treatment of classical organoid lines with conditioned medium from basallike organoids

In addition to treating classical organoids with recombinant OPN, the effect of conditioned media from a basal-like organoid line was also analyzed. For this experiment, the classical PDO18 and medium from PDO42 with a strong basal-like expression profile and high OPN expression and were chosen. Conditioned medium from the classical PDO81 was used as a control. For this experiment, the organoids were seeded at the same time. Except on days when the organoids were passaged, they were treated daily with conditioned medium. The treatment consisted of 500 µl of conditioned medium mixed with 500 µl of tumour organoid medium to ensure the presence of sufficient nutrients and growth factors. Prior to mixing, the conditioned medium was centrifuged to remove any residual cells or debris. The centrifugation step was performed at 4 °C with 1,000 g for 5 min. To determine the response, RNA was isolated at two time points. Simultaneously with the passage of the remaining organoids after one week and finally after two weeks. qPCR analysis was used to compare the control and treated organoids for the expression of classical and basal-like marker genes.

## 2.6 Analysis of OPN treatment in classical organoids using scRNA-seq Single-cell dissociation and sequencing

To further analyze the transcriptional and epigenetic changes induced by OPN in PDAC, a single cell RNA-seq together with single cell ATAC sequencing approach (10X genomics) was chosen. In a previous step, the optimal conditions for OPN treatment were established in two classical organoid lines, PDO18 and PDO81. The culture conditions were kept the same as in the initial test. Therefore, 20,000 cells/50 µl Matrigel cells were seeded for PDO18 and up to 25,000 cells/50 µl Matrigel cells were seeded for PDO81. The organoids were grown in serum-free tumor organoid medium without Wnt supplementation. The organoids were treated every 48 h and passaged after 6 days. The treatment consisted of tumor organoid medium supplemented with 1 µg/ml recombinant human OPN. In addition to the treated organoids, untreated organoids were grown in parallel as a control group. To obtain a sufficient number of cells for the sequencing protocol, up to 2 wells were seeded with 2 Matrigel domes. After a total culture duration of 19 days with 9 treatments the organoids were harvested and prepared for sequencing. Initially the culture medium was removed, and the organoids were mechanically dissociated using pipetting and 1 ml per well of a prewarmed dissociation solution consisting of Accumax (Sigma Aldrich) supplemented with 0.3 mg/ml DNAse I (PanReac AppliChem, Germany). The suspension was transferred to a 15 ml falcon and incubated at 37 °C. The dissociation was continued for up to 60 min and supported by gentle pipetting every 5 min or until a proper dissociation could be observed under the microscope. To stop the dissociation up to 4 ml of the cold washing solution was added. The washing solution consists of basal organoid medium supplemented with 0.04 % BSA (Sigma Aldrich). Subsequently the suspension was centrifuged at 4 °C with 300 g for 5 min. After removing the supernatant, the cells were resuspended and washed in 5 ml of washing buffer before an additional centrifugation step with the same settings. The cells were resuspended in 100 μl of basal organoid medium and counted. For the fluorescence counting 2 μl of Acridine Orange

/Propidium Iodide staining solution were mixed with 18 µl of the cell suspension. 10 µl of the mixture was loaded into a PhotonSlide™ and the cell viability and number were determined using the LUNA-FL™ Dual Fluorescence Cell Counter. For the sequencing, 250,000 cells were pipetted in a protein LoBind 1.5 ml tube and mixed with 1 ml of washing medium. These tubes were then sent to the manufacturer for sequencing. However, it was only possible to harvest 188,000 cells from the treated fraction of PDO81, therefore this lower number was used. The final number of extracted nuclei was around 8.000 per sample.

#### Single-cell data normalization and analysis

The raw scRNA-seq data, obtained from the 10X genomics platform, were processed using the Cell ranger software. In this pipeline the reads were aligned to a reference genome. All further workflows including statistical and graphical representation was conducted in R. For the initial assessment of the results, from this experiment, it was decided to create a pseudo bulk analysis. For this task, the R package aggregateData <sup>76</sup> was chosen. The genes were scaled using the following parameters: cpm > 0.5 and an expression in at least 2 samples. After this scaling step, 18,120 genes remain for further analysis. The chosen normalization method was cyclic loess. With the obtained data it was now possible to perform further analysis. At this point it was possible to create graphs with the normalized expression of certain genes for the different conditions and organoid lines. Since one goal of the analysis was the effect of OPN on the subtype, an artificial subtype classifier was created. This classifier used the published subtype markers <sup>15</sup> where the normalized expression of classical markers was subtracted from the normalized expression of basal-like markers. To investigate the up or down regulation of regulatory pathways three different models were used. On the one hand, SPIA 77 used an enrichment analysis of pathway genes and the KEGG database to determine the perturbation on a given pathway. In this approach the position of the gene in the pathway structure as well as the enrichment is relevant to calculate the significance of the pathway upregulation. For a graphical representation Pathview <sup>78</sup> was used. On the other hand, pathfindeR <sup>79</sup> used information from proteinprotein interactions and tried to map enriched genes on these subnetworks. The active subnetworks are afterwards analyzed for possible underlying pathways. Finally, GOsummaries 80 was used to visualize the Gene Ontology enrichment analysis. This method used a classical over representation approach.

## 2.7 Analysis of the effect of the medium composition on the subtype

The commonly used media is supplemented with a lot of niche factors, which are especially important for organoids with a classical subtype <sup>25</sup>. However, it has been described <sup>81</sup> that these niche factors can modulate the subtype expression in pancreatic cancer organoids to enhance classical subtype expression. Therefore, a basal-like organoid line, PDO100, was chosen to analyze the effect of different media conditions on the subtype. After thawing the organoids were kept in tumor organoid medium without the supplemented Wnt and A83-01. For each condition, a well was seeded with two Matrigel domes with 25.000 cells/50 µl dome. The culture medium was basal tumor organoid medium supplemented with 1x B-27 supplement, 1 mM N-acetylcysteine, 100 ng/ml FGF10 and 10 % RSPO1conditioned medium. Additionally, further niche factors were added depending on the condition A: (EFWsRcNA), 50 ng/ml EGF, 0.5 nM Wnt surrogate, 100 ng/ml Noggin, 500 nM A83-01. B: (EFRcNA), 50 ng/ml EGF, 100 ng/ml Noggin, 500 nM A83-01. C: (EFRc), 50 ng/ml EGF. D (FRcNA) 100 ng/ml Noggin, 500 nM A83-01. The first medium after passage was additionally supplemented with 10 μM Y-27632. An RNA sample was taken at the beginning of the experiment to get a baseline. The organoids were kept in culture for 40 days and were regularly passaged in parallel. At the end of the experiment an RNA sample was taken from each condition and a qPCR was performed.



## 2.8 Analysis of the intracellular protein content

#### Immunofluorescence

For immunofluorescence analysis of OPN and CD44 expression in organoids, standardized protocols were used. 2500 cells were seeded in 5 μl of Matrigel in μ-Slide 8 well (ibidi, Germany). After growing to the desired size, the organoids were fixed in 4% paraformaldehyde for 15 min at room temperature. Afterwards, the organoids were washed three times with 0.75 % Glycine in PBS for 10 min, permeabilized using 0.5 % TritonX100 in PBS and washed three times with IF-wash (0.5 % NaN<sub>3</sub>, 0.2 % TritonX100, 0.5 % Tween-20 and 0.1 % BSA (Fraction V) in PBS) for 10 min. The blocking step was performed with 10 % normal donkey serum (Abcam, United States) in IF-wash for 1 h at room temperature. The primary antibodies were added in blocking solution: anti-OPN (mouse, ab69498, Abcam) with a 1:100 dilution and anti-CD44 (rabbit, HPA005785-100UL, Sigma-Aldrich) with a 1:500 dilution, then incubated over night at 4 °C. The organoids were washed afterwards for three times with IF-wash. The corresponding secondary antibodies were added in blocking solution: anti-mouse (Alexa Fluor™ Plus 555 conjugated, A32773, Invitrogen) with a 1:1000 dilution and anti-rabbit (Alexa Fluor™ Plus 488 conjugated, A32790, Invitrogen) and incubated for 2 h at room temperature in the dark. Following this all steps were conducted at room temperature and in the dark. Two washing steps with IF-wash for 20 min and subsequently two washing steps with PBS for 10 min were done. The nucleus was stained using 300 nM DAPI (Thermo Fisher Scientific) in PBS for 1 h at room temperature. Finally, the organoids were washed with PBS for three times. For imaging a confocal microscope (Nikon, Japan) was used. The final analysis was performed using ImageJ 82.

#### Protein extraction

After removing the culture supernatant, the Matrigel domes with the organoids were rinsed with warm PBS, before being broken down in 1 ml of Cell Recovery Solution (Corning) with complete™ Protease Inhibitor Cocktail (Roche). To all solutions in contact with the cells or protein this protease inhibitor was added. The mixture was transferred to a 1,5 ml tube and incubated for 1 h at 4 °C on a roller. The cells were centrifuged at 500 g, 4 °C for 5 min followed by a washing step with 1 ml cold PBS for two times. After the second washing step all supernatant was discard and the cells were lysed in 55 µl RIPA for 30 min at 4 °C. To remove cell debris the lysate was centrifuged at 14.000 g, 4 °C for 15 min. The supernatant was collected, aliquoted and frozen in liquid nitrogen, before storage at -80 °C.

#### **BCA** Assay

To determine the protein concentration of a sample, a Pierce BCA Assay (Thermo Fisher Scientific) was used. All samples and standards were measured in triplicates. All samples were diluted 1:20 in Milli-Q purified water (MQ). Standards were created with a serial dilution of a 2000 µg/ml BSA stock solution. The BCA color reagent was prepared freshly using a ratio of 50:1 of the reagents A and B. In a 96 well microplate 25 µl of sample or standard was added per well. Afterwards 200 µl of BCA color reagent was added with a multi-channel pipette. The mixture was then incubated at 37 °C for 30 min. The absorbance was measured at 562 nm using a Tecan Spark plate reader (Tecan, switzerland). To calculate the protein concentrations a linear standard curve was created.

#### Western Blot

For Immunoblotting 20 μg protein was loaded onto a NuPage<sup>TM</sup> 4 to 12 % polyacrylamide gel (Thermo Fisher Scientific). The sample was prepared using NuPage™ 4X LDS Sample buffer and NuPage™ 10X sample reducing agent (Thermo Fisher Scientific), for denaturation the mix was heated for 10 min at 70 °C with a following centrifugation step at 10.000 g for 1 min to maintain the volume. For electrophoreses the following settings were used: 5 min with 120 V and 1 h with 180 V using NuPage™ MOPS SDS Running buffer 20X (Thermo Fisher Scientific) as the running buffer. Afterwards were the gels transferred to a PVDF membrane, RTA Mini 0.45 μm LF PVDF (Bio-rad). With a rapid protein transfer apparatus, the Trans Blot Turbo (Bio-rad), it was possible to blot within 30 min at 25 V.

Afterwards the membrane was washed for 5 min in Tris-buffered saline (TBS). All washing steps were performed on a shaker. If it was necessary to control the blotting efficacy, the membrane was reversibly stained with a 0,1 % ponceau red solution. To remove the staining, the membrane was washed multiple times in MQ or 0,1 M NaOH. The membrane was blocked for 1 h with 5 % nonfat dry milk powder in Tris-buffered saline with 0,1 % Tween 20 (TBS-T). Prior to incubation with the primary antibody (AB), the membrane was washed for 3 times with TBS-T for 5 min. The primary antibody was diluted in 5 % nonfat dry milk. The incubation of the membrane with the prim. AB was performed over night at 4 °C. On the next day, 3 washes with TBS-T for 5 min were executed before the membrane was incubated with the species-specific secondary antibody horseradish peroxidase conjugated, diluted in 5 % nonfat dry milk. Afterwards further 3 washes with TBS-T were conducted. Finally, the membrane was visualized using Pierce™ ECL Western Blotting Substrate (Thermo Fisher Scientific) and imaged using the VILBER FUSION FX (VILBER, France).

## Antibody list The following primary antibodies were used for western blot analysis of protein samples.

Target	Host species	Antibody	Company	Dilution
Osteopontin	Mouse	ab69498	Abcam	1:500
Kreatin 17	Mouse	MA1-06325	Invitrogen	1:500
GATA6	Rabbit	5851S	Cell Signaling Technology	1:2000
Vinculin	Rabbit	13901S	Cell Signaling Technology	1:1000

The following secondary antibodies conjugated with HRP were used for western blot analysis.

Target	Antibody	Company
Mouse IgG	ab6789	Abcam
Rabbit IgG	ab97051	Abcam

## 2.9 Analysis of the extracellular protein content **ELISA**

The OPN protein levels in organoid culture supernatant were measured using the ELISA kit DOST00 (R&D Systems) according to the manufacturer's instructions. Each sample was assayed in duplicates. Organoids were cultured until a sufficient density was reached. The supernatant was collected after 72 hours of culture and frozen at -80 °C until use. To normalize for different cell densities among the organoid cultures, lysates were taken and the protein content was determined. The supernatant was thawed only once, prior to use. Possible cell debris was removed by a prior centrifugation step: 10 min, 4 °C with 500 g. To acquire readings in the measuring range it was necessary to dilute some of sample with assay diluent RD5-24 up to 1:100. Standards were created with a serial dilution of a 200 ng/ml stock solution of rec. OPN with assay diluent RD5-24. To each of the wells (coated with monoclonal anti-OPN antibodies) 100 μl assay diluent RD1-6 was pipetted. After adding 50 μl of sample or standard to the wells, the plate was incubated for 2 hours at room temperature. Afterwards, unbound OPN was washed away using a washing buffer provided by the kit. Thereafter 200 µl of an enzyme linked OPN conjugate solution was added to each well and the plate was incubated for further 2 hours at room temperature. Subsequent to the final washing step, 200 µl of a substrate solution was pipetted to the wells. After 30 minutes the reaction was stopped with the addition of 50 μl of stopping solution, provided by the kit. Hereinafter the optical density was measured at 450 nm with a wavelength correction at 540 nm using a Tecan Plate reader. To calculate the corresponding concentrations a standard curve with a 4-PL fit was created. The normalized OPN concentrations [ng/ml/µg] were obtained by dividing them with the matched protein amount.

### Cytokine Array

For the expression analysis of 80 different cytokines in organoid culture supernatants were measured using the Cytokine Array kit ab133998 (abcam) according to the manufacturer's instructions. Organoids were seeded with a density of 30.000 cells / 50 µl Matrigel. For each line 2 wells (12WP) with 2 Matrigel domes were seeded. The medium was exchanged after one day in culture. The supernatant from both wells were collected and pooled after 72 hours of culture and immediately used. To remove debris the supernatant was centrifuged at 15.000 g for 10 min at 4 °C. If necessary, reagents were reconstituted prior to use, in order to prepare a 1X working solution according to the manufacturer's instructions. At the beginning, the array membrane was placed in 2 ml blocking solution for 30 minutes at room temperature with the printed side up. For each membrane, a separated chamber in a provided 8-well tray was used. Afterwards the blocking solution was aspirated and 1 ml of the sample was added. For a strong signal, the sample was incubated overnight at 4 °C. To minimize background signals an optional large volume wash was conducted after the overnight incubation. For this wash the membrane was placed in 20 ml of 1X Wash Buffer I and shaken at room temperature for 45 min. In addition to the large volume wash, the membrane was washed respectively three times in 2 ml of 1X Wash Buffer I and two times in 2 ml of 1X Wash Buffer II for 5 minutes at room temperature. This washing procedure was performed after every overnight incubation. Thereafter the membrane was incubated in 1 ml of 1X Biotin-Conjugated Anti-Cytokines at 4 °C overnight. After aspirating the Anti-Cytokine solution from the well and executing of the washing procedure, 2 ml of the 1X HRP-Conjugated Streptavidin solution was pipetted to the membrane for a final overnight incubation at 4 °C. After a final washing step, the membrane was transferred to a plastic sheet and wetted with 500 µl of a 1:1 mix of Detection Buffer C and Detection Buffer D. After 2 minutes of incubation at room temperature the chemo luminescence detection was performed on a FUSION FX. To analyze relative differences in the expression profile of the organoid cohort, densitometry was conducted using ImageJ with the Protein Array Analyzer. To correct for background signal, the mean summed signal intensities from the negative control spots was subtracted from each markers summed signal intensities. To normalize data across different membranes, one membrane was dedicated to being the reference membrane. The other arrays were normalized using the average summed signal intensities of the positive control spots. Finally, the normalized signal intensities were used to create a z-score for each cytokine.

## 2.10 Analysis of gene expression

#### **RNA** extraction

For RNA extraction, organoids were cultured until they reached the required density. If samples from the same PDO line were to be compared, all organoids were cultured in the same way. This means that the medium exchange and passages were performed simultaneously and the RNA was harvested at the same time. Prior to harvesting, the organoids in the Matrigel domes were washed with warm PBS. The Matrigel domes were then transferred to a 1.5 ml DNA LoBind tube. At this point, the organoids could either be snap frozen in liquid nitrogen or proceeded directly to RNA extraction. The RNeasy Plus Micro Kit (Qiagen, The Netherlands) was used for RNA extraction according to the manufacturer's instructions. The following reagents are included in the kit. First, organoids were lysed in 350 μl RLT Plus buffer and transferred directly to a gDNA elimination column. The column was then centrifuged at 8,000 g for 30 s and 300 µl of 70 % ethanol was added to the filtrate. The resulting mixture was transferred to a RNeasy MinElute Spin Column and centrifuged for 20 s at 8,000 g. The flowthrough was discarded and the column was washed with 700 μl of RW1 buffer followed by 500 μl of RPE buffer using the previous centrifugation procedure. Prior to elution, a final washing step was performed with 500 µl of 80 % ethanol and centrifugation at 8,000 g for 2 min. After discarding the supernatant, a further centrifugation step at 20,000 g for 5 min was performed to dry the membrane. The RNA was eluted into a 1.5 ml tube at 20,000 g for 1 min using 14 µl of RNAse-free water. The RNA concentration was measured using the NanoDrop (ThermoFisher) and the RNA was then stored at -80 °C before further use.

#### qPCR

To analyze the RNA expression by qPCR a reverse transcription step was necessary. For this process, the GoTaq 2-step RT-qPCR system (Promega, United States) was used. In a first step the RNA and primers were denaturized. Since long genes, with qPCR primers located on the first exon, were analyzed, both Oligo(dT)<sub>15</sub> and Random primers were used. For all experiments an RNA amount of 600 ng was chosen. Since only exon spanning qPCR primer pairs were used, no reverse transcriptase control was not used. For each reaction 1 μl Oligo(dT)<sub>15</sub> Primers, 1 μl Random primers, 600 ng RNA and nuclease free water to a final volume of 10 µl are added in a 1,5 ml DNA LoBind tube on ice. In a SmartBlock (Eppendorf, Germany) the mixture was heated to 70 °C for 5 min and then again kept in ice for additional 5 min. Afterwards 10 μl of the reverse transcriptase mix was added. This mixture consists of: 1,5 μl nuclease free water, 4 μl GoScript 5X Reaction Buffer, 2 μl MgCl<sub>2</sub>, 1 μl PCR Nucleotide Mix, 0,5 μl Recombinant RNasin Ribonuclease Inhibitor and 1 μl GoScript Reverse Transcriptase. To keep the volume, the tube was spun down in a microcentrifuge. Using the SmartBlock a temperature protocol with 25 °C for 5 min, 42 °C for 1 h and finally 72 °C for 15 min was used. The resulting cDNA was afterwards stored at -20 °C. For qPCR Analysis the cDNA was diluted 1:20. Each sample was measured in triplicates. Per well 4 µl of the diluted sample was loaded into the MicroAmp optical 96 well plate (ThermoFischer, United Staes) together with 5 μl of the GoTaq qPCR Master Mix 2X and 1 μl primer pair (final concentration 400 – 500 nM). The 96 well plate was then covered with a MicroAmp optical adhesive film to prevent evaporation and well to well contamination. To perform the qPCR a 7500 Fast Real-Time PCR System (ThermoFisher) was used. The thermal cycling parameters were programmed in the following way: 2 min at 95 °C for polymerase activation and then 40 cycles with 95 °C for 15 s for denaturation and 60 °C for 60 s for annealing and extension. Afterwards the melting curve was analyzed to determine the quality of the amplicon. Only samples with the right melting curve were further analyzed. For analysis and calculation of the CT-value the software included within the 7500 Fast Real-Time PCR System was used. As a first step, the baseline and the threshold for each gene was chosen. Afterwards the CT value was determined. For each sample and gene of interest the arithmetic mean was calculated. Using the mean the  $\Delta\Delta$ CT value was calculated as shown in equation 1.

Equation 1: calculating the  $\Delta\Delta$ CT value:

$$\Delta \Delta CT = (CT_g - CT_c)_{treated \ sample} - (CT_g - CT_c)_{control \ sample}$$

CT of the gene of interest  $CT_q$ 

geometric mean of the CT from the control genes: GAPDH and HPRT1  $CT_c$ 

treatment sample analyzed sample

control sample sample towards the others were normalizes to

Afterwards the fold change was calculated using equation 2.

Equation 2: Calculation of the fold change:

$$RQ = 2^{-\Delta \Delta CT}$$



### List of Oligonucleotides

The following Primers were used for qPCR analysis.

Target	forward	reverse
GAPDH	GTTCGTCATGGGTGTGAACC	GCATGGACTGTGGTCATGAGT
HPRT1	GCCAGACTTTGTTGGATTTG	TGAACTCTCATCTTAGGCTTTG
SPP1	GGTCACTGATTTTCCCACGG	CTCCTCGCTTTCCATGTGTG
GATA6	TCAAAGACTTGCTCTGGTAATAGC	CCCGCACCAGTCATCACC
KRT15	CCAGGATGCCAAGATGGCTG	TGGGAAGAAACCACCTGTCC
FGFBP1	TGCTCAGAACAAGGTGAACGC	ACCACTTTGCTGTGAAGTCCA
AGR2	CCTGATGGCCAGTATGTCCC	TTCATGTTGTCAAGCAACAGAGC
TFF1	GTCCCTCCAGAAGAGGAGTGT	GGACTAATCACCGTGCTGGG
CD44	ACACAAATGGCTGGTACGTCT	CCGTGGTGTGGTTGAAATGG
c-Met	TGGGCACCGAAAGATAAACCT	TCGGACTTTGCTAGTGCCTC
MMP9	CATTCAGGGAGACGCCCATT	AACCGAGTTGGAACCACGAC
PLAU	CCTGCTTCTCTGCGTCCTG	CCATTCCCCTCATAGCAGGT

The following gRNA were used with CRISPR/cas9

Target	Sequence
SPP1	AGGCATCACCTGTGCCATAC
non-targeting	GTATTACTGATATTGGTGGG

The following primer was used to amplify the CRSPR/cas9 cut site in the SPP1 gene.

Target	forward	reverse	
SPP1	TCCCTTTCCCTTGCCTAATAGT	TGCACCTCTCGCCATAATTG	

#### 2.11 Plasmid constructs

In order to obtain the same plasmid backbone containing the gRNA for both CRISPR/Cas9 systems, a cloning step had to be carried out. For the expression of the CRISPR/Cas9 system the plasmid pX330 would be used. The plasmid containing the gRNA for SPP1 was already prepared. Additionally, a plasmid containing the gRNA for the non-targeting control would be cloned. In a first step the Oligos (Sigma Aldrich) with the information of the gRNA were annealed. Therefore, a mixture containing 1 µl of sense and antisense 100 mM oligos, 1 μl 10x T4 Ligation Buffer (NEB) and 7 μl of nuclease free water was incubated in a PCR thermocycler for 30 min at 95 °C. After cooling to 25 °C at rate of 5 °C/min, 190 µl of nuclease free water were added. In a next step the annealed gRNA was ligated into a previously digested pX330 backbone. For this reaction, 50 ng of the digested pX330 backbone were mixed with 1 µl of the annealed oligos, 5 µl of 2x Quick Ligase Buffer (NEB), 1 µl of Quick Ligase (NEB) and nuclease free water to make a total volume of 10 µl. This reaction is homogenized and incubated at 4 °C over night. Now 5-alpha Competent E. coli (NEB) could be transformed with the ligated plasmid. For this step 50  $\mu$ l of the thawed bacteria suspension was gently mixed with 1  $\mu$ l of the plasmid. The cells were transformed using the heat shock method: After 30 min on ice, the mixture was transferred to a 42 °C water-bath for 30 s and afterwards the mix was incubated for further 2 min on ice. After adding 950  $\mu$ l of pre warmed SOC-Medium the mixture was incubated at 37 °C for 1 h on a shaker. Around 30 µl of the mixture were plated on a prewarmed LB-amp plate under sterile conditions. The plate was incubated over night at 37 °C. On the next day, a few colonies were picked and cultivated in 5 ml of LB-amp at 37 °C in a shaker. After 16 h, 1.8 ml of the culture medium was harvested using a



centrifugation step at 6,000 g for 15 min at 4 °C. The pellet was further processed to plasmid preparation using a Miniprep (Qiagen) kit. The following reagents were included in the kit. The pellet was resuspended in 250 µl buffer P1. Afterwards the cells were lysed in 250 µl of Buffer P2 for up to 5 min. To stop the reaction 350 µl of pre-cooled buffer N3 was added. The suspension was centrifuged for 10 min at 18,000 g. The supernatant was transferred to a QIAprep spin column 2.0 and centrifuged for 60 s. The flowthrough was discarded, and the spin column was washed using 500 μl of buffer PB and a centrifugation for 60 s. Another washing step is conducted using 750 μl of buffer PE and another centrifugation step. To remove any residual buffer, the empty column is spined down for 60 s. The Plasmids are finally eluted into a fresh 1.5 ml tube using 50 µl of nuclease free water. After an incubating the column for 1 min, the DNA is eluted in a final centrifugation step. To verify the inclusion of the target gRNA into the vector, the plasmid was sent to Eurofins Genomics for Sanger Sequencing.

#### 2.12 Statistical analysis

For analytical and graphical representation, GraphPad Prism was used. Additionally, R was used for statistical and graphical representation of scRNA-seq data. Two tailed T-tests were used whenever appropriate. Previous calculations would be carried out in Microsoft Excel. The z-distribution was calculated using equation 3:

Equation 3: Calculation of the z-distribution:

$$score = \frac{(expr. - mean \ expr.)}{SD}$$

calculated score in the z-distribution score

expression of the gene/cytokine of the selected sample expr. mean expression of the gene / cytokine sample for all samples mean expr.

standard deviation of the gene/cytokine expression for all samples SD



## 3. Results

## 3.1 Selecting appropriate PDAC organoid lines based on subtype identity

The PDAC organoid cohort used as part of this thesis was previously established and characterized at the European Pancreas Center, in Heidelberg, Germany<sup>21,35</sup>. Using previous RNA-seq data <sup>35</sup> SPP1 was identified as a top hit in a differential expression analysis between the classical and the basal-like organoids (Fig. 2 - A and B). Especially interesting is the result, that SPP1 is one of the most significant and strongly upregulated genes in basal-like organoid cohort. Surprisingly, the significance is much stronger compared with the classical subtype regulate gene GATA6 (Fig. 2 - C). Based on these preliminary results, we next selected a cohort of organoid lines based on their transcriptomic subtype and SPP1 expression profile. The initial experimental aims were twofold. On one hand, classical organoid lines were to be treated with recombinant OPN. For this purpose, organoids with a strong classical subtype expression and low OPN expression were desired. On the other hand, establishing a SPP1 knock-out in a basal-like organoid line with a high baseline SPP1 was aimed for. Other considered parameters were TP53 depletion, since the presence of wildtype TP53 has been reported to induce cell death after CRISPR-mediated double strand DNA breaks 83. This led to the choice of PDO18 and PDO81 as classical organoid lines and PDO55, PDO100 and PDO42 as basal-like organoid lines. Based on RNA-seq, PDO42 exhibited the strongest OPN expression and the weakest classical subtype scores (Fig. 2 - D). The tumor from which PDO42 was created, was classified as an anaplastic tumor, showing marked dedifferentiation.

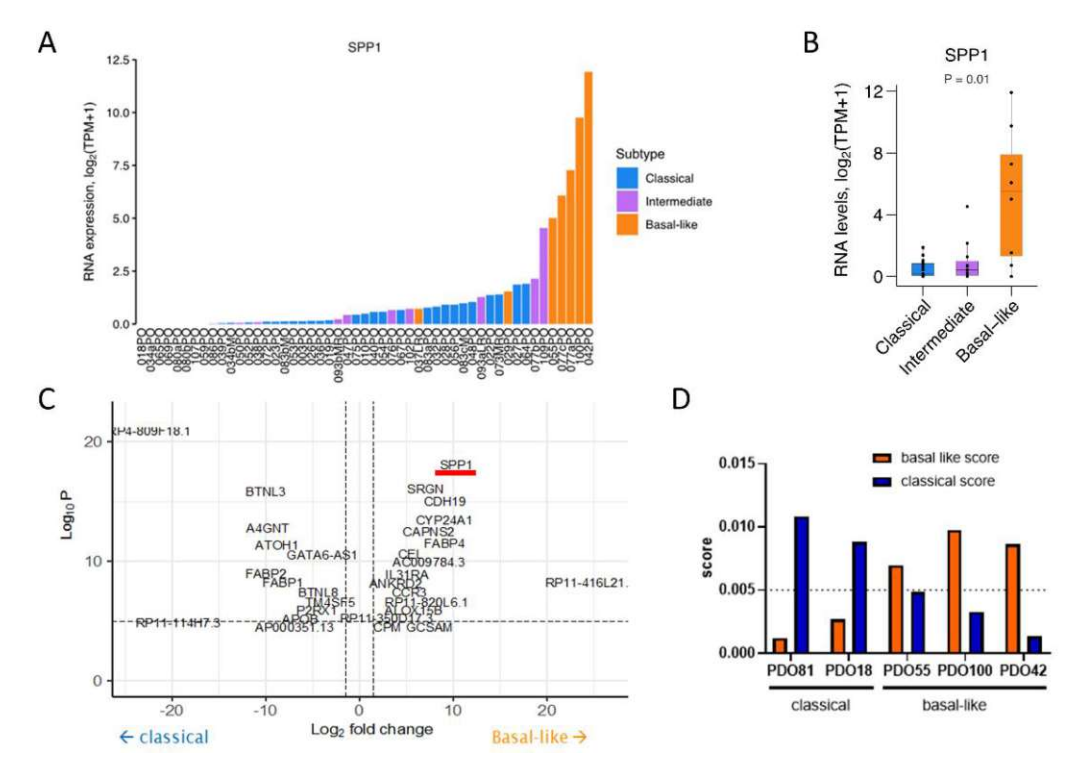


Figure 2: Processed RNA-seq data from the established organoid cohort created by 35. A, OPN expression by different organoids. B, corellation of OPN expression and organoid subtype. C, differential expression analysis between the classical and basal-like subtype. D, Analysis of subtype scores from pre-selected organoids.

## 3.2 Verification of the RNA sequencing results Analysis on the RNA level

The first experimental step was to verify the results from the RNA-seq 35 using the preselected organoid lines. Since the data was from an RNA-seq obtained at earlier organoid passage numbers than in the experiments, the first experiment was the analysis of the expression of two subtype markers (one classical and one basal-like) and SPP1 on the mRNA level. Additionally, the CD44 expression, an important OPN receptor was analyzed.

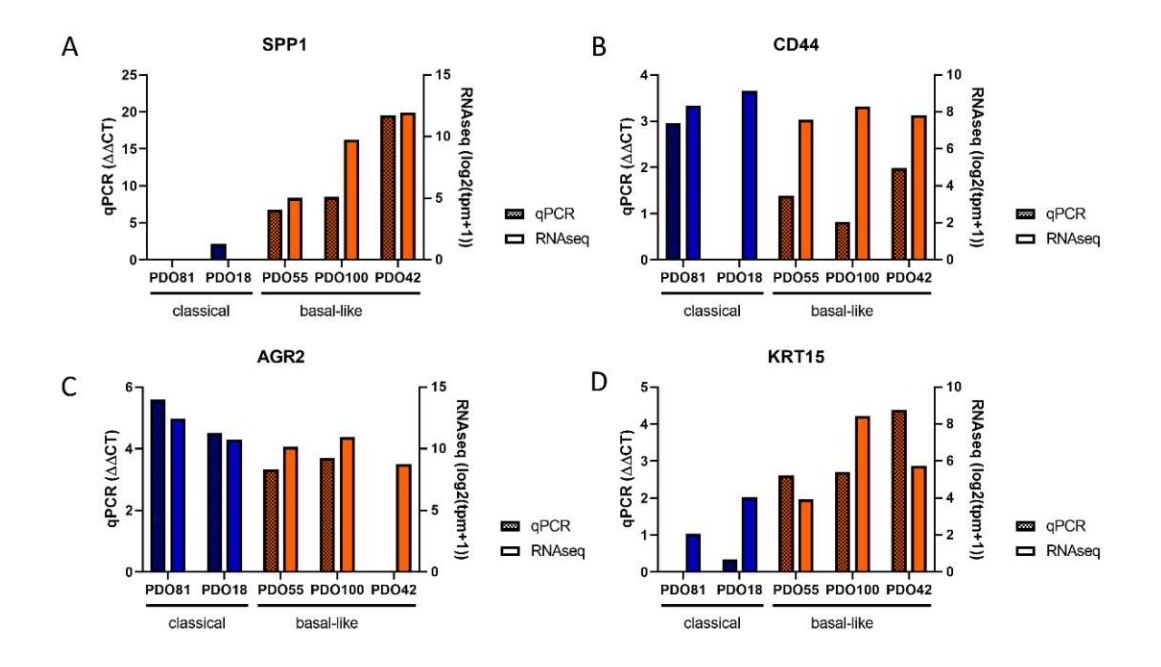


Figure 3: Analysis of the organoid cohort regarding subtype marker and OPN expression. The qPCR results are ddCT values measured against the organoid line with the least expression, therefore one is always zero. A - D, comparison of RNA-seq data 35 with qPCR data for the different organoid lines: SPP1 (A), CD44 (B), AGR2 (C) and KRT15 (D).

This analysis verified the basic results from the RNA-seq 35. The classical organoid lines show a much weaker SPP1 expression compared to the basal-like organoid lines. Among the basal-like organoid line PDO42 shows by far the strongest SPP1 expression. Regarding the subtype marker expression, both classical organoid lines show a strong classical marker and a weak basal-like marker expression. Surprisingly, the basal-like organoid lines, except for PDO42, show a strong classical marker expression as well. PDO42 seemed to show the strongest basal-like signature with a high basal-like marker expression and a weak classical marker expression (Fig. 3 - B and C). With the high SPP1 expression, this makes it the obvious choice for a proof-of-concept SPP1 KO experiment. For the treatment of classical organoids with recombinant OPN the presence of OPN receptors is essential. Therefore, the expression of CD44 was analyzed as well. The qPCR showed for all organoid line comparable expression levels, showing the utility of both classical organoid lines for this experiment.

## Analysis at the protein level

Since the correlation between RNA and protein expression can vary widely in human cells 84, the protein expression of OPN was analyzed as well. OPN is a soluble protein which is mostly found in cell culture supernatant. However, the qualitative analysis by western blot is much faster and cheaper using intercellular protein, therefore this was conducted as well. For quantitative analysis, an ELISA using cell culture medium was performed.

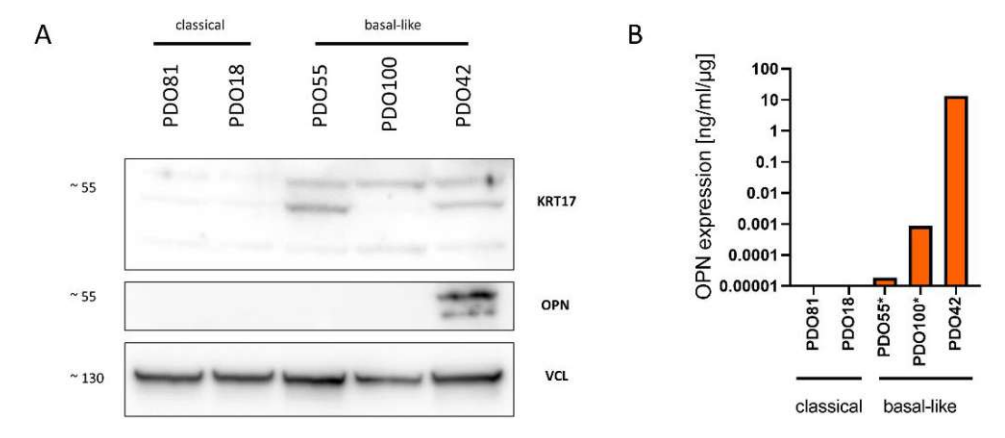


Figure 4: Analysis of the organoid cohort regarding protein expression. A, Analysis of intracellular protein expression, using western blot. Vinculin was used as a loading control. B, Analysis of the extracellular OPN expression (the OPN conc. for the samples from PDO55 and PDO100 was below the standard curve and had to be extrapolated). Total protein was used for normalisation.

The western blot (Fig. 4 - A) showed the intracellular protein levels of OPN and KRT17. It was only possible to observe OPN in PDO42, confirming the qPCR results, which showed the highest SPP1 expression in PDO42. KRT17, a basal-like marker protein, shows a differential expression between the different subtypes of the organoids. The quantitative analysis of secreted OPN with an ELISA assay (Fig. 4 - B), showed an extraordinarily strong OPN expression by PDO42. For the other basal-like organoid lines, the OPN concentration in the cell culture medium was much lower, hence the measured OPN concentration was below the standard curve and had to be extrapolated. In conclusion it can be observed that PDO42 shows a basal-like signature on the RNA level, and consistent protein expression. Additionally, PDO42 showed the highest OPN expression, both intra- and extracellularly. As it was reasoned that a loss of SPP1 should have a stronger phenotype in a OPN high expressing line, PDO42 was selected to establish a SPP1 KO line.

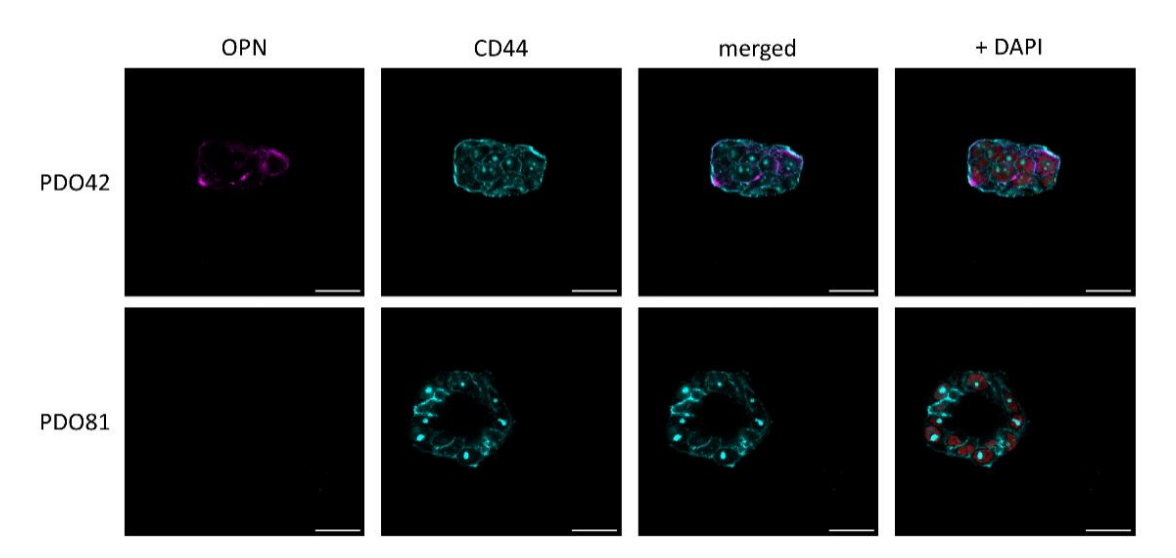


Figure 5: Comparison of a basal-like OPN expressing organoid (PDO42) with a classical organoid (POD81). Confocal IF analysis of formalin fixed organoids. Possible co-localisaton of OPN at its receptor CD44 in white. Scale bar represents 25 μm.

Another interesting point is the localization of OPN inside the organoids. One question would be, whether OPN is co-localized with its receptor CD44. Using immunofluorescence (IF), expression of OPN in PDO42 was confirmed while the classical line PDO81 failed to exhibit OPN expression (Fig. 5). However, a merged image with CD44 only showed partial overlap, indicating only limited presence of OPN in close proximity to the receptor.

#### Secretome analysis in classical versus basal-like organoids

Cytokines released by tumor cells play a vital role in modulating the TME and can influence tumor progression <sup>85</sup>. Due to the importance of cytokine expression an exploratory analysis of the secretome profile based on the transcriptomic subtype was performed.

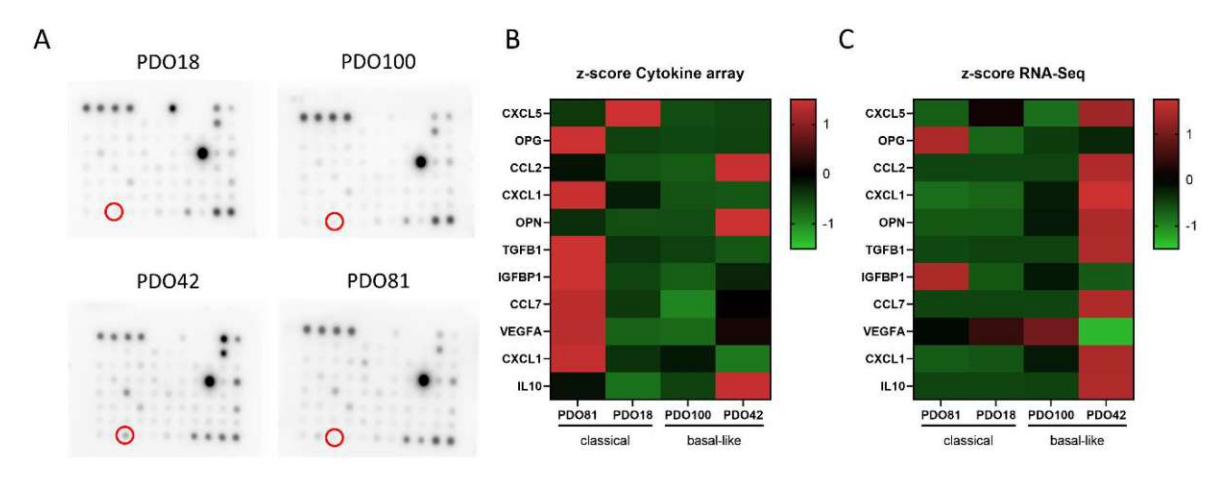


Figure 6: Analysis of the organoid cohort regarding secreted protein expression. A, Human Cytokine Array using media from different organoid lines (red circle OPN). B, z-score of the expression difference of the most differently expressed cytokines based on the cytokine array. Quantification was based on a densometric analysis. C, z-score of the expression difference of the same cytokines based on RNA-seq.

The cytokine array contained 80 human cytokines, among them OPN (Fig. 6 - A). Again, only PDO42 showed a strong OPN signal. The cytokine expression was quantified and is represented as a z-score among the organoids. Since an absolute quantification was not possible, the cytokines with the strongest differential expression were chosen for this analysis (Fig. 6 - B). A similar z-score was created using the RNA-seq data for the same organoids and cytokines (Fig. 6 - C) 35. Surprisingly, PDO81 exhibited the strongest overall cytokine expression.



Using the GEPIA2 52 dataset I compared the highest 25 % of cytokine gene expressing tumors, with the lowest 25 %, calculating a hazard ratio for each cytokine gene. Most of these cytokines do not show a significant high hazard ratio except for CXCL5 (2.4), OPN (2.4) and CCL7 (1.9). The comparison between the results from the cytokine array and the RNA-seq, shows a major difference: The cytokine expression of PDO81 is much stronger and the cytokine expression of PDO100 and PDO42 is much weaker than expected. Whereas the RNA-seq data generally show a high cytokine expression in the basal-like organoids, this cannot be observed in the cytokine array. Only for a few specific cytokines (CCL2, OPN and IL10) showed PDO42 the strongest expression.

## 3.3 CRISPR/Cas9 mediated SPP1 Knock Out in PDO42 Establishment of a SPP1 KO organoid line

As described previously, PDO42 was selected to establish a SPP1 KO line. The necessary gRNAs have been previously designed and cloned. An electroporation-based plasmid delivery system was used for transfection in the PDO42 line. After an antibiotic based selection step, a bulk SPP1 KO organoid line was created. To obtain clean results and to prevent an overgrowth of unedited cells, it was necessary to create a clonal homozygote SPP1 KO line. The two clonal lines were isolated from the bulk SPP1 KO line using serial dilutions. Thus, there were in total 4 organoid lines, derived from the wild type PDO42. A previously published scrambled gRNAs was used as a control for non-specific effects of CRISPR/Cas9

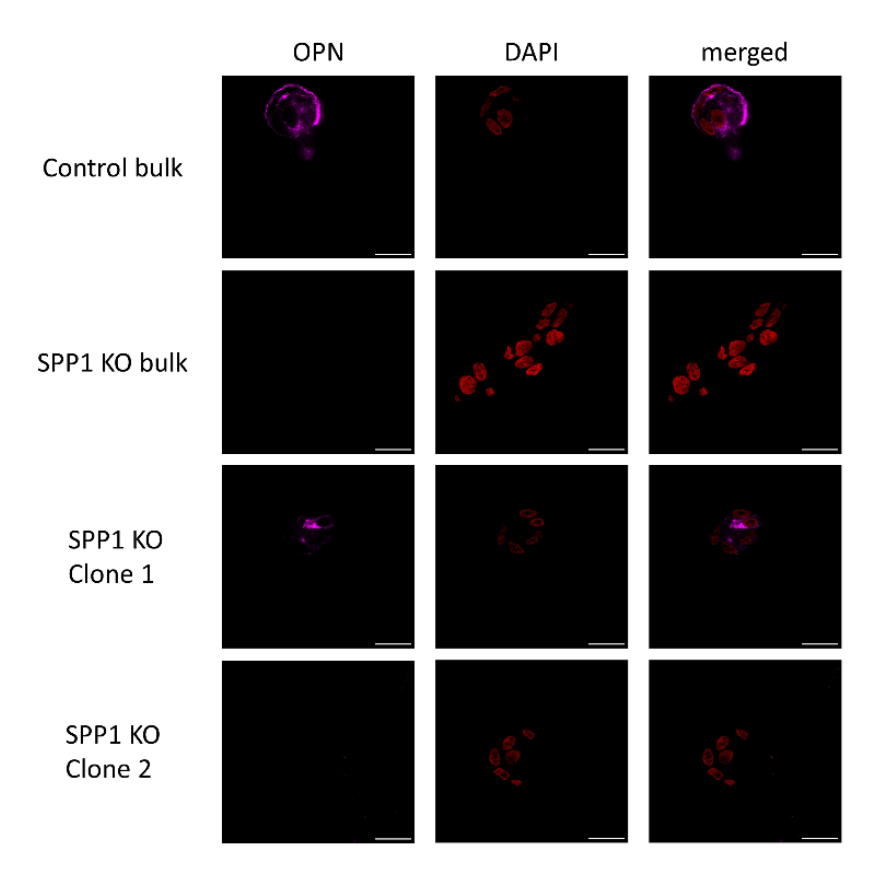


Figure 7: Comparison of the OPN expression in the CRISPR cohort derived from PDO 42. Confocal IF analysis of formalin fixed organoids. OPN is only present in the control bulk and in the clone 1. Scale bar represents 25  $\mu m$ .

Initial validation of KO was performed using IF (Fig. 7). IF showed, that OPN was only present in the control bulk and in clone 1. With this initial result clone 2 seemed to be a promising candidate for further experiments utilizing the SPP1 KO. To further analyze the KO efficiency DNA was isolated from the KO bulk and from clone 1. The SPP1 gene with the CRISPR/Cas9 cut site was sequenced and further



analyzed using the ICE Tool 75. The Analysis showed in case of clone 1: CRISPR/Cas9 did induce a INDEL in both alleles, however one allele showed a 3 bp deletion. Therefore, no frameshift mutation was induced, and functional protein could still be translated. In case of the KO bulk, a high KO efficiency of 97 % was calculated. To validate the SPP1 KO on the protein level a western blot was performed (Fig. 8 - A). No OPN was be observed in the SPP1 KO clone 1 and bulk. For the quantitative analysis of secreted OPN an ELISA was performed (Fig. 8 - B). Again, no OPN was detectable in the cell culture medium from clone 2. Since no OPN was detectable on the protein level and we were interested in the functions mediated by the OPN protein, it was not necessary to validate the KO any further by an analysis of the genomic cut site.

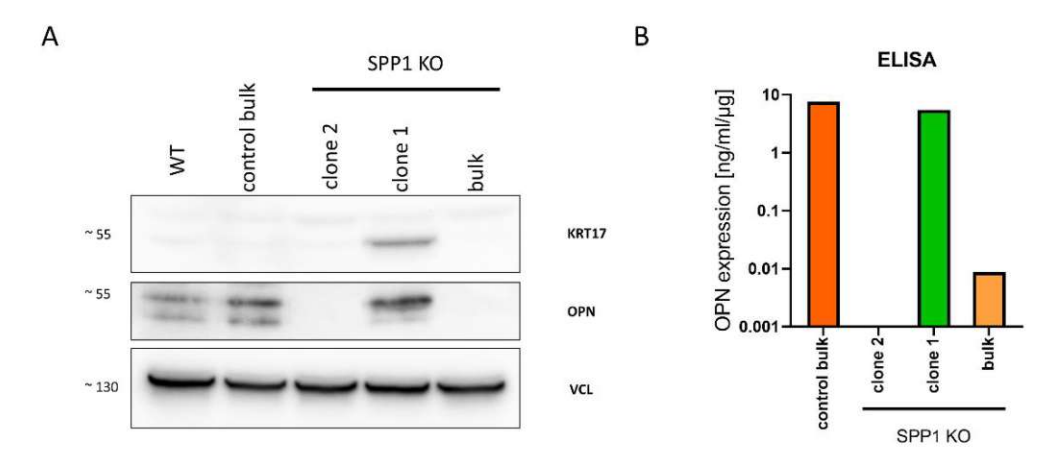


Figure 8: Comparison of the OPN expression in the CRISPR cohort derived from PDO 42. A, Analysis of intracellular protein expression, using western blot. Vinculin was used as a loading control. B, Analysis of the extracellular OPN expression using ELISA. Total protein was used for normalisation.

These findings confirm previous results from the IF. Clone 1 only shows a slightly decreased OPN expression, compared with the control bulk. Interestingly, the SPP1 KO bulk had a decreased OPN expression by 3 orders of magnitude. Whereas with the data from the DNA analysis, such a strong effect would not have been expected. Due to strong decrease of OPN expression the SPP1 KO bulk was included in the further experiments.

## An SPP1 KO in a basal-like organoid line shows an effect on subtype markers

The most interesting property of OPN lies within its potential role of modulating the PDAC subtype 1. Therefore, the expression of selected subtype marker and other genes of interest was analyzed by qPCR.

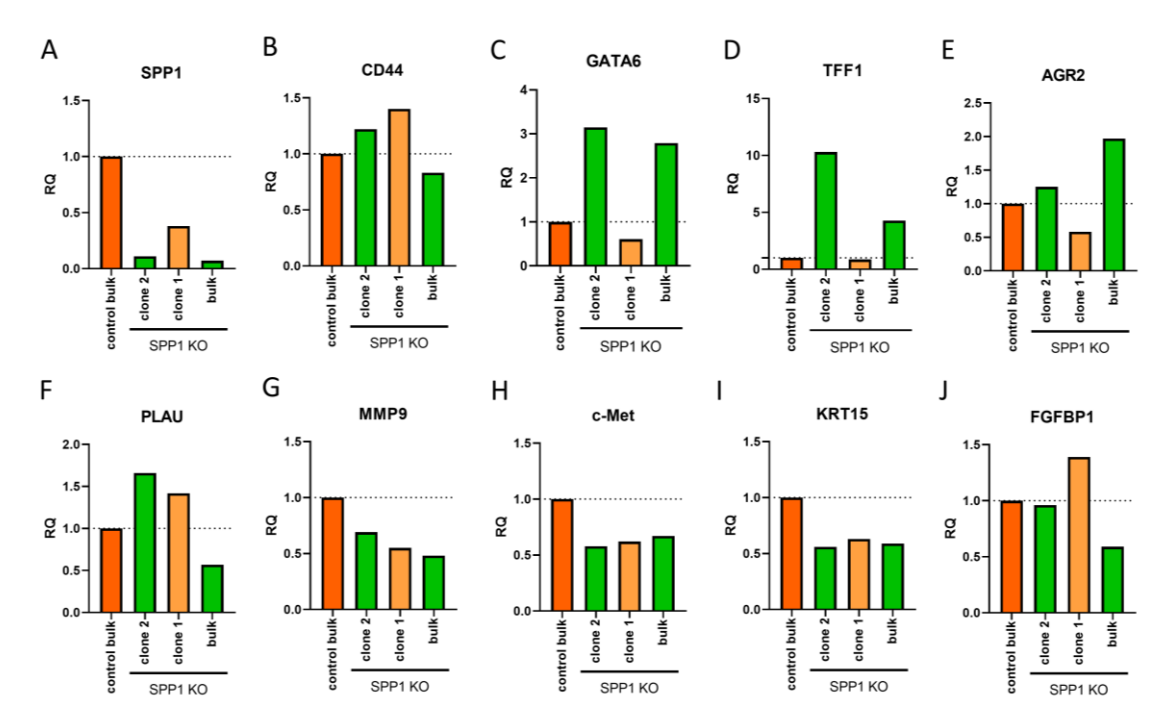


Figure 9: Comparison of gene expression in the CRISPR cohort derived from PDO42. The difference of marker expression between control bulk and the other organoids was analysed using qPCR. All samples were measured in triplicates. A, SPP1 expression. B, CD44 expression. C-E, classical subtype marker: GATA6, regulator (C), TFF1 (D), AGR2 (E). F-G, OPN downstream targets: PLAU (F), MMP9 (G). H-J, basal-like subtype marker: c-Met, regulator (H), KRT15 (I), FGFBP1 (J).

Expectedly, SPP1 expression was decreased in the SPP1 KO lines (Fig. 9 - A). With the remaining RNAlevels a KO on the protein level is still feasible, since after a frameshift only truncated protein would be translated. As expected, the expression in clone 1 is reduced, but not as much as in the other clonal KO line, where a homozygote KO had occurred. The expression of the OPN receptor CD44 also showed no response to the SPP1 KO (Fig. 9 - B). An SPP1 KO in a basal-like organoid lead to an increase in classical marker expression (Fig. 9 - C - E). Especially the classical regulator GATA6 and the marker TFF1 showed a strong upregulation. Interestingly, the clone 1 where the OPN is still present, did not show any upregulation. The basal-like subtype markers did not respond in a comparable way to the SPP1 KO (Fig. 9 - H - J). Only a partial decrease can be observed, which is as well present in clone 1. The OPN downstream genes PLAU and MMP9 did not show a strong response to the KO of SPP1 (Fig. 9 - F & G). These downstream targets were selected, based on literature and an analysis of expression in the organoid cohort 87,88.

#### An SPP1 KO is not associated with chemotherapy resistance in vitro

I next investigated possible effects of the SPP1 KO regarding chemotherapeutic sensitivity. For this, 3 common chemotherapeutic agents used in the treatment of PDAC were selected. They resemble the main components from FOLFIRINOX: 5-flourouracil (5-FU), SN-38 the active component of irinotecan, and oxaliplatin. The experiment was conducted in 3 organoid lines: the wildtype PDO42, non-targeting control PDO42 (control) and the SPP1 KO clone 2 PDO42.

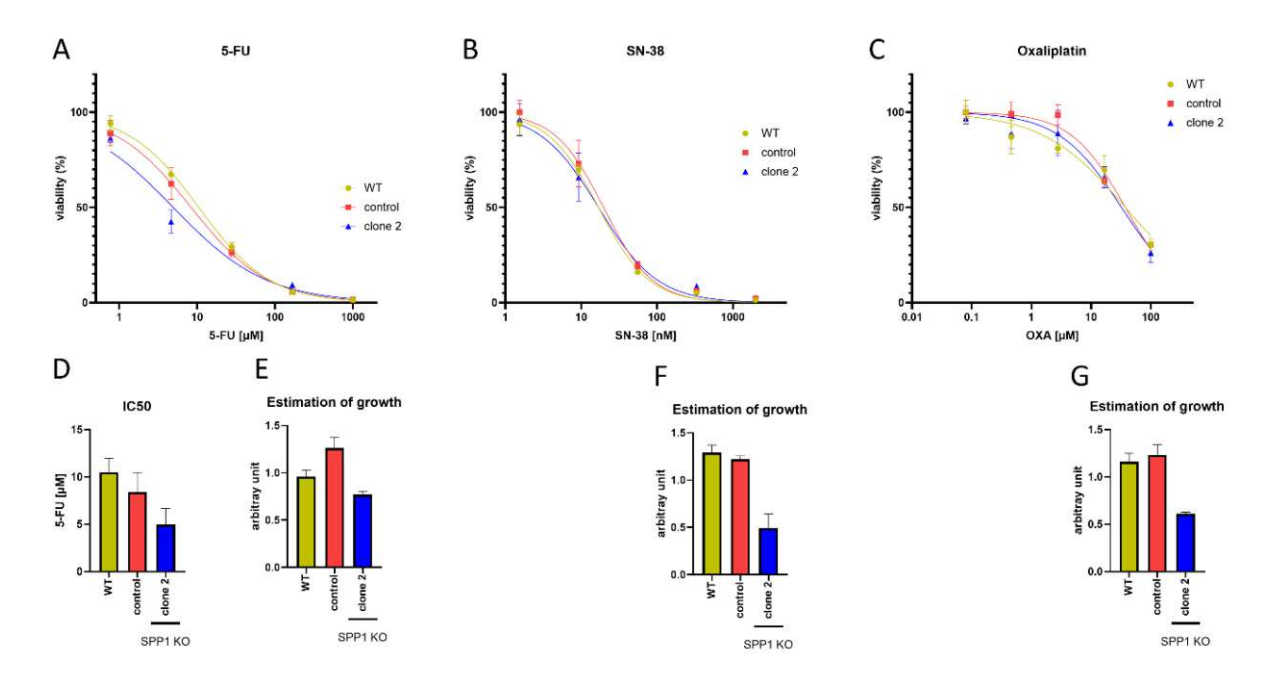


Figure 10: Organoid response to chemotherapy treatment is not linked to OPN expression. A - C, Dose response curve for treatment with 5-FU (A), SN-38 (B) and oxaliplatin (C) on three organoid cultures derived from PDO42. D, IC<sub>50</sub> for treatment with 5-FU (confidence intervall (CI) = 95%). E-G, growth estimates of different organoid lines at the end of the experiment, obtained from the respective control wells from the plates with 5-FU (E), SN-38 (F) and oxaliplatin (G). (for all conditions n =

The viability of the organoids was determined at the end of the experiment, after 72 h of drug treatment and a further 72 h of drug washout (Fig. 10 - A - C). Only for 5-FU it was possible to observe a slight increase in chemotherapy resistance. Using the measurements, a half maximum inhibitory concentration (IC<sub>50</sub>) was calculated for the 5-FU treatment (Fig. 10 - D). The IC<sub>50</sub> as well showed a slight increase in chemotherapy resistance of clone 2 compared to control or WT. However, this result is only supported by a single measurement point. Using the non-treated control wells of the experiment, it was possible to compare the growth of the different organoid lines. As already observed during culture of this line, clone 2 expands slower (Fig. 10 - E - G).

#### 3.4 Treatment of classical organoids with recombinant OPN

Apart from establishing a SPP1 KO in a basal-like organoid line, assessing possible effects on subtype identity using exogenous OPN in classical organoids was another central part of my thesis. First, different OPN treatment conditions were evaluated to find a robust response, which were then further explored using single-cell RNA sequencing (scRNA-seq).

#### Exogenous OPN induces a shift of subtype markers in classical organoids

The two classical organoid lines PDO81 and PDO18 were selected to investigate the effects of exogenous OPN on subtype identity. The initial conditions for the OPN treatment were derived from previous experiment in the literature <sup>1</sup>.

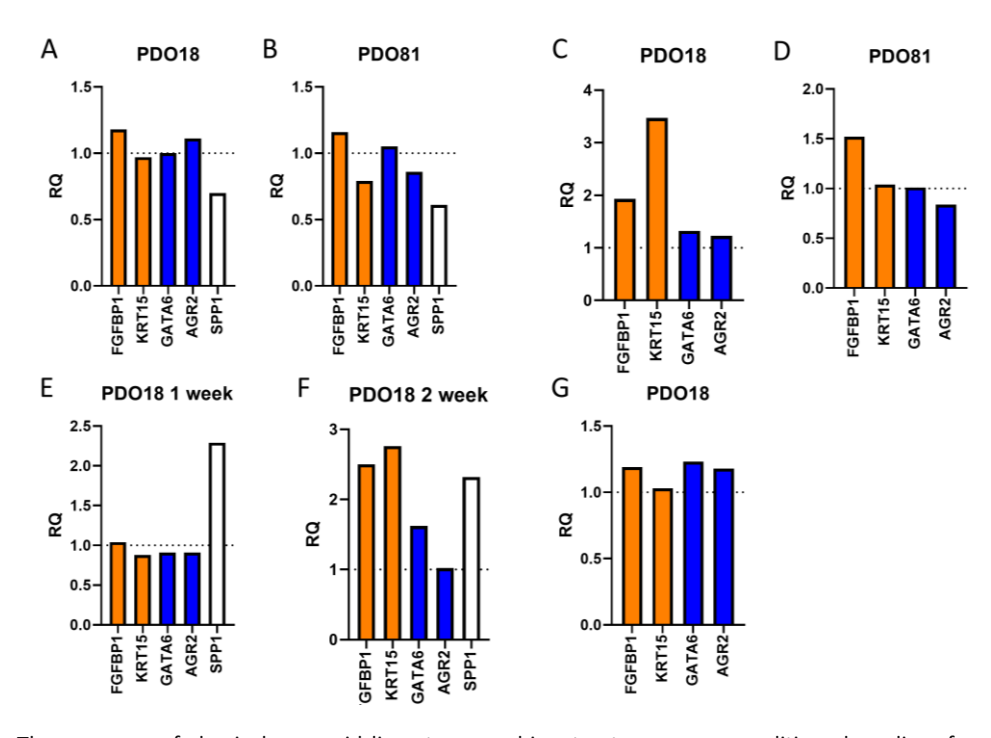


Figure 11: The response of classical organoid lines to recombinant osteopeon or conditioned medium from a basal-like organoid line. The difference of marker expression between treated and untreated organoids was analysed using qPCR. All samples were measured in triplicates (basal-like subype markers are depicted in orange and classical subtype markers are depicted in blue). A-B, 1 week culture duration with three treatments of 0.5 µg/ml OPN: PDO18 (A), PDO81 (B). C-D, 3 week culture duration with nine treatments of 1 µg/ml OPN: PDO18 (C), PDO81 (D). E-F, conditioned media experiment using medium from basal-like PDO42 and classical PDO81 as control for one week (E) and two weeks (F). G, a repetition of the conditions shown in C, used for scRNA-seq.

An initial treatment of in total 3x 0.5 µg/ml OPN did not show any obvious marker response (Fig. 11 - A & B). Increasing the number of treatments and dosage of OPN to a total of 9x 1 μg/ml resulted in an increase in basal-like markers (Fig. 11 - C & D). Especially in PDO18 OPN induced a strong marked response as quantified by qPCR. Notable is the absence of a response among the classical markers. This treatment condition could induce a shift of the basal-like markers; therefore, it was decided to further investigate the effect using scRNA-seq.

The basal-like organoid line PDO42 showed a high expression of secreted OPN. Therefore, I wanted to determine whether conditioned medium from PDO42 could induce a similar subtype shift in a classical organoid line. The classical organoid line PDO18 was cultured in tumor organoid medium consisting of 50 % conditioned medium containing secreted components from either basal-like PDO42 or classical PDO81 as a control. The medium was obtained from parallel cultures of the respective organoid line. The subtype marker response was measured at two timepoints: after one and after two weeks (Fig. 11 - E & F). After the second timepoint the basal-like subtype marker expression increased, suggesting a subtype modulating effect of basal-like cell culture supernatant.

## Investigation of subtype markers using single cell RNA sequencing upon treatment with recombinant OPN in a classical organoid line

To better understand the effect of OPN on classical organoids, the treatment shown in (Fig. 11 - C & D) was repeated organoids from an earlier passage. However, in this case the results were additionally evaluated using scRNA-seq. Notably, the growth rate of organoids treated with OPN was strongly decreased. During the last passage before analysis, 25.000 cells were seeded for PDO81. After six days in culture the treated organoids expanded to 190.000 cells whereas the untreated organoids grew much stronger to 525.000 cells. For PDO18 a similar growth difference could be observed. In a first analysis the effect on PDO18 was analyzed using qPCR. However, the previously observed modulation of subtype markers could not be confirmed in this experiment (Fig. 11 - G).

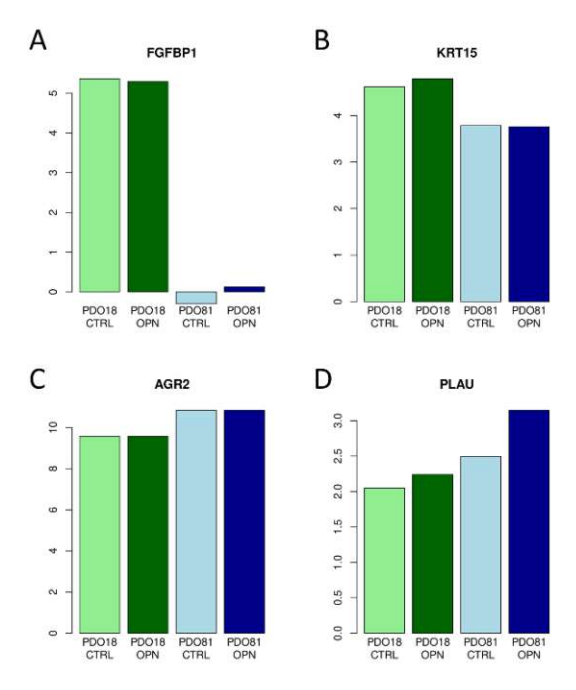


Figure 12: Validation of the qPCR data of OPN-treated classical organoids with data obtained from bulk scRNA-seq analysis and analysis of a potential subtype shift. A-C, Comparison of normalised transcrips of subtype marker for both organoid lines in the treated (OPN) and untreated group (CTRL), FGFBP1 basal-like marker (A), KRT15 basal-like marker (B) and AGR2 classical marker (C). D, PLAU OPN downstream marker (significant upregulation p < 0.05).

An initial analysis of the scRNA-seq data could be included in this thesis. For this purpose, a pseudo bulk dataset was created and analyzed. The effect of OPN on subtype markers determined by qPCR (Fig. 11 - G) could be validated (Fig. 12 - A - C).



In addition to the limited number of subtype markers assessed by qPCR, an artificial classifier using all subtype markers from Moffit et al 15 was created. For this classifier, the normalized expression of classical markers was subtracted from the normalized expression of basal-like markers. Using this classifier, it was possible to see a slight increase of a basal-like signature (Fig. 13 - C). Consistent with the initial subtype scores (Fig. 2 - A), PDO81 had a stronger classical signature compared to PDO18.

With a gene set enrichment analysis (GSEA) it was possible to see, that a few upregulated basal-like subtype markers were mostly responsible for the changes in the classifier (Fig. 13 - D). The most strongly upregulated basal-like markers were CST6 and KRT17 (Fig. 13 - A & B). The PLAU gene showed an upregulation as well, consistent with being a known OPN downstream target and suggesting the presence of exogenous OPN (Fig. 12 - D).

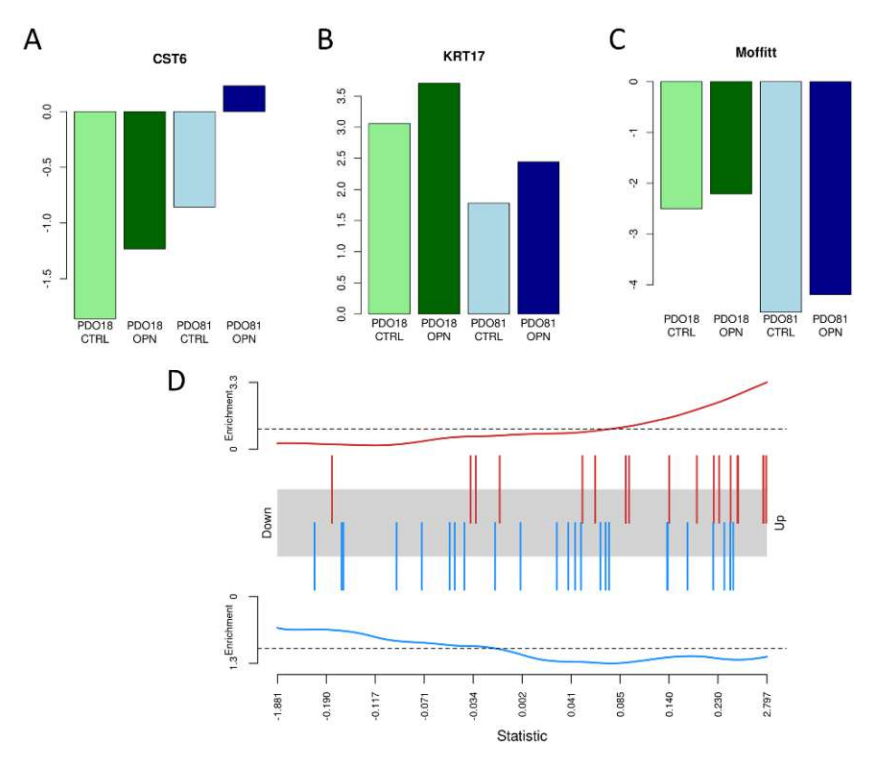


Figure 13: Analysis of scRNA-seq data utilizing a pseudo bulk: A-B Chosen basal-like subtype markers with a strong response (P < 0.05). C, artificial classifier using moffits subtype marker (p=0.056). D, GSEA using Moffits subtype marker: basal-like markers in red and classical markers in blue.



### Pathway analysis of pseudo bulk scRNA-seq data

For further analysis of the OPN-induced interactions, a pathway analysis was performed. For this task, a several different approaches were conducted. The analysis was based on the pseudo bulk scRNAseq. First, a signaling pathway impact analysis (SPIA) was conducted. SPIA is a combination of a classical gene enrichment analysis and analysis of the perturbation caused by the enrichment. Using a bootstrap procedure, it is possible to calculate the significance of the determined pathway perturbation <sup>77</sup>. The SPIA analysis showed 5 significantly upregulated pathways (Fig. 14 - A).

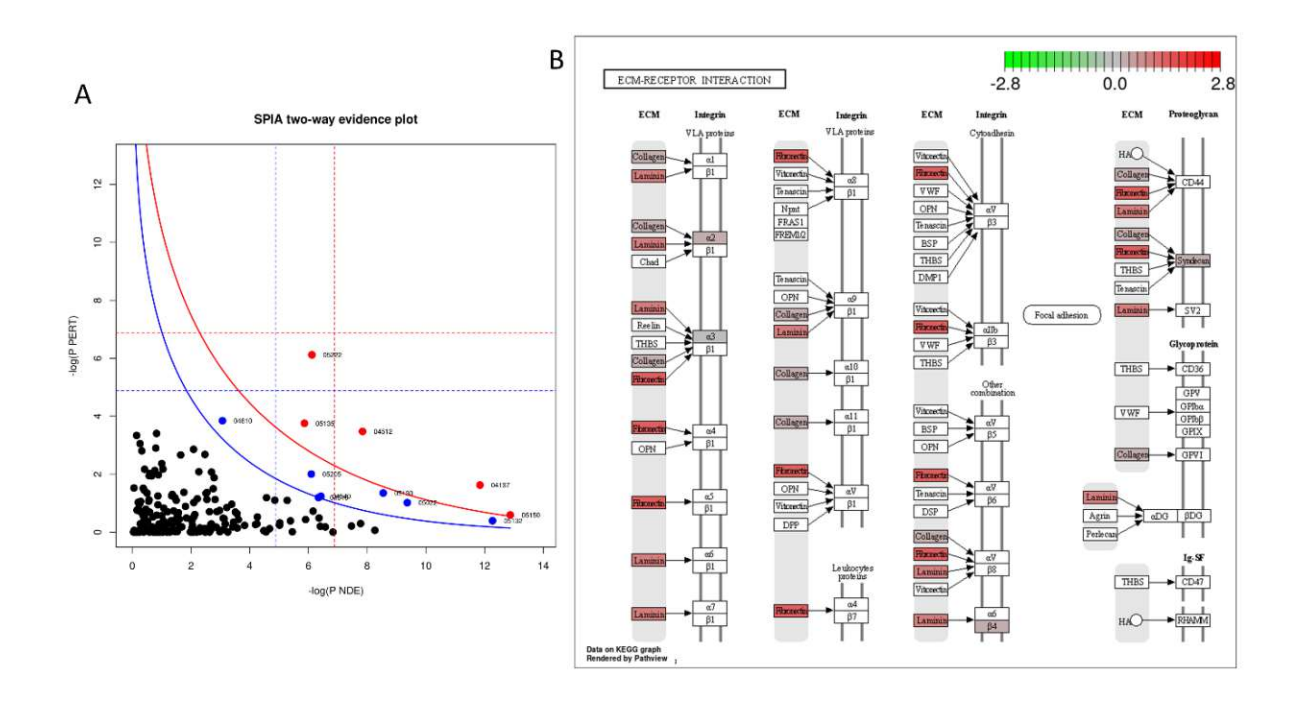


Figure 14: Analysis of pathway regulation of OPN treated classical organoids using the bulk scRNA-seq data. A, SPIA shows 5 upregulated KEGG pathways (p < 0.05) (pERT for the pertubations accumulation and pNDE for the overrepresentation). B one chosen representation of a upregulated pathway rendered by pathview 78 (ECM receptor interaction).

The three most significantly upregulated pathways were: small cell lung cancer, ECM-receptor interaction and mitophagy (Fig. 14. - B). Other pathways attributed to the infections with different bacteria or viruses with decreasing significance were found. However, these pathways were not considered for further analysis as both up- and downregulation was observed. The most notable perturbation in the detected pathways was the upregulation of ECM receptor interactions. Since OPN can bind to many different receptors, this upregulation is not unexpected. Interestingly, the mitophagy pathway was detected among the upregulated pathways as well. Mitophagy is the process where primarily damaged mitochondria are degraded. Mitochondria can be damaged by the formation of reactive oxygen species, due to leakage of electrons in the electron transport chain 89. Mitophagy itself is not described so far to be induced by OPN. However, there are reports of the induction of autophagy by OPN promoting chemotherapy resistance in hepatocellular or pancreatic cancer <sup>90,91</sup>.

Next, Gene Ontology (GO) enrichment analysis was conducted (Fig. 15 - A). With this tool the upregulated genes could be associated with GO terms. OPN itself is associated with the following GO terms: ossification and cell adhesion 92. Surprisingly, the most significant and strongest upregulated terms were part of the leucocyte activation or degranulation pathways. OPN is known to maintain an important role in inflammatory response, but mostly in the recruitment and not in the degranulation of leukocyte <sup>51,93</sup>. Beside this, other GO terms included cell adhesion molecule binding, adherens junction, and cell substrate junction. These terms are connected to either integrin binding (a OPN receptor) or ECM cell interactions. A weak upregulation of the MET signaling, a potential basal-like regulator, was found as well.

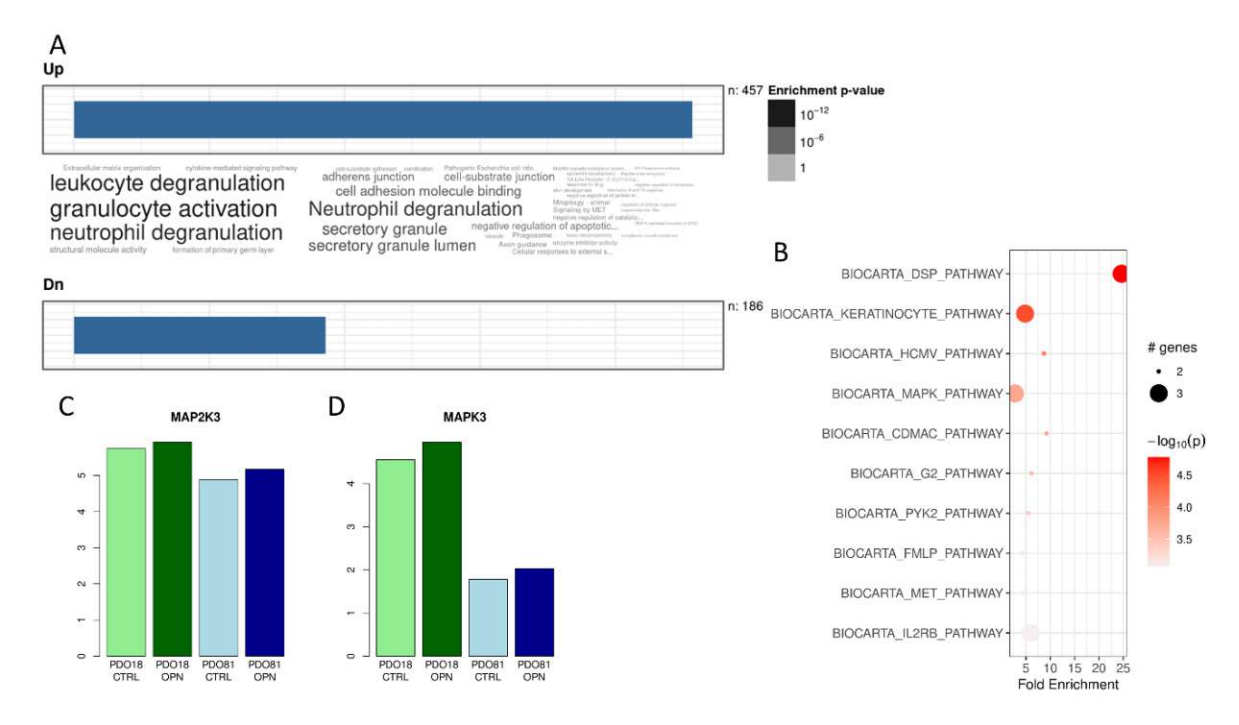


Figure 15: Analysis of pathway regulation of OPN treated classical organoids using the bulk scRNA-seq data. A, over representation analysis using the GO dataset. B, Pathfinder Analysis. C-D most relevant genes used in the pathfinder analysis: MAP2K3 (C), MAPK3 (D).

Finally, a Pathfinder analysis was conducted, which tries to find enriched subnetworks and annotates them to Biocarta pathways (Fig. 15 - B). The strongest enriched pathway was the DSP pathway. It describes the regulation of MAP kinase (MAPKs) pathways through dual specificity phosphatase (MKPs). The dual specificity MKPs are known for their negative regulatory function towards MAPKs 94. Surprisingly, the MAPK pathway was found to be enriched as well. Other enriched pathways are associated with cell differentiation in the epidermis, viral reprogramming or induction of DNA synthesis. A more matching upregulation would be again the MET pathway. However, the analyses using pathfinder must be viewed with great caution, since the upregulation of pathways are based on only two or three genes. The two most common ones are MAP2K3 and MAPK3. As it can be seen (Fig. 15 C & D), the enrichment is also not strongly manifested.

# 3.5 Effects on media composition on PDAC subtype in organoid cultures

Patient derived tumor organoids are dependent on a niche factor rich medium. However, organoids vary in the dependence on these niche factors. In particular, classical organoids depend on WNT or R-Spondin 1. A KO of the classical regulator GATA6 was previously shown to decrease this dependency <sup>72</sup>. However, it is unknown how a basal-like organoid line which is not as dependent on these factors would respond to long term culture in a niche factor rich medium. So far, only a slight decrease of the basal-like signature has been reported <sup>35</sup>.

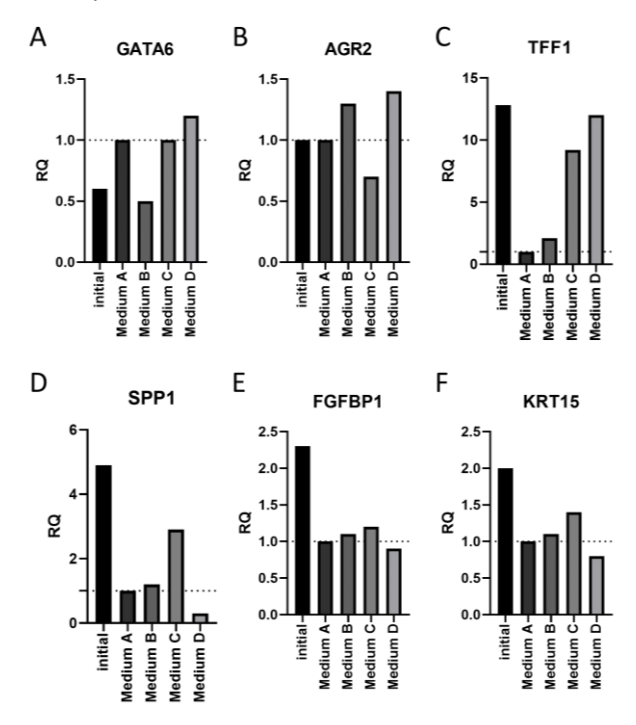


Figure 16: The effect of different media conditions on the subtype of an PDAC organoid. For this experiment one organoid line PDO100 was kept for 40 days in different media conditions. A: EFWsRcNA, B: EFRcNA, C: EFRc, D: FRcNA. The difference of marker expression was analyzed using qPCR. All samples were normalized towards medium A, the classical tumor organoid medium. All samples were measured in triplicates. A-C, classical subtype marker expression GATA6 (A), AGR2 (B), TFF1 (C). D, SPP1 expression. E-F, basal-like marker expression FGFBP1 (E), KRT15 (F).

For this experiment, the basal-like organoid line PDO100 was chosen. It was cultured in four different media compositions for 40 days. The different media conditions were: A - normal tumor organoid media; B - tumor organoid media without WNT; C - tumor organoid media without WNT, Noggin and A83-01; D - tumor organoid medium without WNT and EGF. RNA was collected at the beginning and at the end of the period. The expression of subtype markers and SPP1 was analyzed using qPCR (Fig. 16). Both basal-like subtype markers were down regulated after 40 days. This effect occurred at a similar rate for all the different medium conditions. With an exception to TFF1, the classical markers seem to be more stable. In particular TFF1 and SPP1 show large differences in downregulation between the different media. Apparently, the removal of WNT alone is not enough to keep a stable SPP1 expression. Especially the removal of EGF reduced the expression of SPP1, this effect is supported by literature 95. The most differently expressed marker was TFF1, especially medium A and B induced a strong downregulation. This result surprises, since TFF1 was assumed to be upregulated by EGF 96. Medium D, without EGF, appears to maintain the most stable TFF1 expression. In addition to the analysis by qPCR the growth of the organoids in the different conditions was monitored as well. Most notably was the strongly reduced growth in medium D. This organoid culture had to be stopped after 40 days, whereas the other media conditions did not prevent a further culture period.

# 4. Discussion

In this thesis I conducted multiple experiments to elucidate the influence of OPN on transcriptomic subtypes in PDAC. These subtypes are a focus of increased research, as evidence indicates a role in sensitivity to standard chemotherapy regimens and patient prognosis <sup>14–16,33,35</sup>. The experiments were conducted using multiple previously established patient-derived pancreatic cancer organoid lines. These organoids retain the transcriptional and genomic heterogeneity of the corresponding tumors and have been shown to model the chemotherapeutic response of the respective patient <sup>21,35</sup>. In these organoid lines SPP1 was one of the most strongly differentially expressed genes between subtypes. Thus indicating the importance of SPP1 in context of PDAC subtypes.

## 4.1 Analysis of the organoid cohort

### Validation of previous characterizations of the organoid cohort

Initially, I verified the results from the RNA-seq using five preselected organoid lines. Most important was the level of SPP1 expression and a stable subtype expression. Therefore, I analyzed the subtype marker and SPP1 expression using qPCR. Additionally, OPN expression was quantified on the protein level using ELISA. Although the results show some differences in the expression pattern (e.g. CD44 expression, or the extent of the basal-like signature in PDO100) the overall trend is preserved. A plausible reason for the deviation from the RNA-seq data is that the sequencing was uniformly performed at early passage numbers, whereas the passage number of the organoid cohort used in the experiments differed between the individual lines. In conclusion, PDO42 exhibited the most pronounced basal-like signature together with the highest OPN expression and was therefore chosen for the SPP1 KO experiment. Both classical organoids PDO18 and PDO81 did not express OPN, and both maintained a strong classical signature. Therefore, both organoids were used in further experiments whether OPN can induce basal-like signature.

#### Analysis of secreted cytokines

Secreted factors can influence the tumors growth and the tumor microenvironment. For example TGFβ is associated with the suppression of apoptotic pathways or EMT induction <sup>97</sup>. OPN, studied in this thesis, also belongs to the cytokine family. The analysis of the results of a cytokine array with medium from four organoid lines showed unexpected results. Out of the four organoids analyzed, half were of the basal-like subtype (PDO42, PDO100), and the other half were of the classical subtype (PDO18, PDO81). In contrast to the literature and the results from the RNA-seq, the cytokine expression did not show any correlation between a basal-like signature and a high cytokine expression 98. Especially PDO81 showed a surprisingly high cytokine expression. Unfortunately, from the analyzed cytokines only the OPN expression was verified using ELISA and qPCR. Therefore, it is unclear, if PDO81 actually expressed such high cytokine concentrations or whether problems in the experimental design led to these results. Possible issues in the experimental setup are the impossibility to achieve the same cell number in the experiment due to different growth rates and the normalization step, which might have induced an overrepresentation of PDO81. The basal-like organoids in this cohort showed a slower growth rate, indicating a possible underrepresentation of their cytokine expression.

# 4.2 OPN ablation in a basal-like organoid upregulates classical subtype markers Subtype modulation

The created SPP1 KO lines derived from PDO42 showed a strong upregulation of the classical subtype markers. Differences in the upregulation between the clonal and the bulk line may come from the reduced heterogeneity in the clonal line or the general variability, however the general trend of an upregulation of classical markers is unambiguous. Interestingly, the decrease of the basal-like markers is not as strong and is as well present in clone 2, where only a heterozygote SPP1 KO \*/- occurred. Either a slight reduced OPN expression alone can affect the basal-like makers, or the resulting

downregulation was not significant. The comparison with previous results, how strongly the SPP1 KO has changed the subtype, is difficult. Most articles use different scorings system based on RNA-seq data which cannot be directly compared to qPCR data <sup>18,20,35</sup>.

Notably, only a few subtype markers were analyzed in the qPCR. In order to gain a complete picture of the induced subtype modulation by an SPP1 KO, an RNA-seq approach could be used. With RNA-seq data, it would be possible to create classifiers to quantify the subtype change <sup>15</sup>. Furthermore, it would be possible to analyze which pathways are up- or downregulated after the SPP1 KO. Additionally, it would be interesting to see, how strongly the EMT signature was reduced, since EMT suppression is associated in-vivo with an increased chemotherapy response 99. Additionally previous studies showed a decreased growth in-vivo using tumor xenografts after an SPP1 KO 1. Therefore, experiments with a tumor organoid xenograft could provide further insight whether OPN ablation would have a clinical significance.

To further validate the subtype modulating effects of OPN, it would be necessary to create a SPP1 rescue in a SPP1 KO organoid line.

#### An SPP1 Ko does not affect Chemotherapy resistance

It was reported that a basal-like subtype is associated with a poor chemotherapy response in the clinic<sup>33</sup>. To further analyze if an SPP1 KO mediated subtype shift would affect the chemotherapy resistance, a drug test was performed. In the used organoid cohort, derived from PDO42 (WT, control and SPP1 KO) a strong correlation between the subtype scores and chemotherapy resistance was not observed. This pattern, where basal-like organoids were not associated with a higher chemotherapy resistance, could be observed in other organoid cohorts as well <sup>34</sup>. Additionally, SPP1 was previously not among the genes associated with chemotherapy resistance 35. Therefore the results are in line with this. Despite an increase in the classical signature observed in the SPP1 KO compared to the wildtype line, no significant effect on chemotherapy sensitivity was observed. This suggests that the higher chemotherapy resistance of basal-like PDAC in-vivo might be modulated by the TME and not merely mediated by tumor cell-intrinsic properties. To further analyze the effect of an SPP1 KO on TME interactions, experiments with tumor organoid xenografts or co-cultures could be performed. Each of these models have different drawbacks. A xenograft lacks the right immune system and co-culture experiments cannot account for all different cell types present in the TME. However, it is still necessary to better understand how the basal-like subtype provides its in-vivo chemotherapy resistance, which is apparently not always preserved in an in-vitro model.

During the drug treatment the growth rate of the non-treated wells was observed as well. It is possible to see, that SPP1 KO clone 2 had a decreased growth rate, compared to the other lines. The difference in the growth rates was previously observed in-vitro in a SPP1 KO in KP4 cells 1. However, the growth of an KP4 SPP1 KO xenograft model showed an even stronger decrease, indicating that OPN is a major growth regulator in basal-like cells <sup>1</sup>. A further research question would be if the same effect would occur with an organoid model.

## 4.3 Treatment of classical organoids with OPN

Initially different treatment conditions were analyzed to find a condition were OPN induced a subtype shift. Nine treatments with 1 µg/ml OPN induced an upregulation of basal-like subtype markers in the classical organoid lines PDO18 and PDO81. This means the organoids needed a much longer treatment duration, compared with Capan-2 cells 1. Interestingly, only the basal-like subtype markers were upregulated, whereas the classical subtype markers did not show a difference in their expression pattern. This result surprises, since the SPP1 KO mostly affected the classical subtype markers, and not the basal-like subtype markers. However, especially GATA6 should be modulated as well since it is known for its role in the blockade of EMT or subtype shift <sup>17,72</sup>. Thus, unchanged GATA6 expression



could limit the duration of the effect from OPN. However, only a limited number of subtype markers were analyzed using qPCR. Additionally, the PDO18 line exhibited a much stronger response to the OPN treatment compared to the PDO81 line. A possible explanation would be, that PDO18 has already a higher basal-like signature and is therefore more susceptible for subtype alternations. In a reported experiment involving co-cultures using CAFs and PDAC organoids, the subtype of organoids characterized as grade 2 (a mostly classical subtype with basal-like features) could be modulated in contrast to the highly classical organoids, where a subtype modulation was not possible <sup>25</sup>.

To gain further insides in the mechanisms of a subtype modulation by OPN in classical organoids, the treatment experiment was repeated, with a scRNA-seq as a readout. Unfortunately, during the repetition of the experiment, no strong subtype shift occurred. Without the subtype-shift the results from the pathway analysis cannot show possible OPN interactions leading to a subtype shift. For example, it would have been interesting to find out if OPN would induce EMT and which pathways are affected in PDAC, since for other tumor entities these interactions have been described <sup>3</sup>. It was possible to use the scRNA-seq data to create a pseudo bulk mimicking RNA-seq data. With this data it was possible to investigate the outcome. Beside the missing effect on the tumor subtype OPN exerted an effect: Firstly the OPN downstream target PLAU was upregulated. Secondly multiple upregulated pathways are known be influenced by OPN. Thirdly, a strong growth difference between the treated and untreated cohort occurred and finally a slight increase in the basal-like signature could be observed. It seems like OPN interacted with the tumor cells but did not induce a strong subtype shift. While the anticipated effect was not observed, it is essential to consider potential factors that may have influenced the outcome. For example, a fresh batch of OPN and freshly thawed organoids were used in the repeat experiment and could have affected the outcome. Another explanation for the results could be the contamination of the organoid lines. Since the organoids were kept in sterile conditions with a culture medium containing Primocin a bacterial contamination is highly unlikely. Furthermore, frequent visual inspections should have revealed a possible contamination. The theory of a contamination would be supported by the presence of multiple pathways associated with different infections. However, since these pathways do not show significance and are found to be up and downregulated, the implications are unclear. To rule out the unlikely possibility of a viral infection, the sequencing data could be specifically analyzed for unaligned reads and possible different taxa than homo sapiens <sup>100</sup>.

In summary, OPN can increase the basal-like signature in classical organoids. However, the magnitude and the mechanisms behind are still unclear.

# 4.4 Conditioned medium from a basal-like organoid line can modify the subtype in a classical organoid line

Beside the treatment of classical organoids with recombinant OPN, I treated classical PDO18 with conditioned medium from the basal-like PDO42. The question was if, secreted factors from a basal-like organoid line can induce a basal-like signature in a classical organoid line. The conditioned medium induced an increase of basal-like subtype markers, comparable to the OPN treatment. Interestingly, as was observed with shorter OPN treatments, the effect only occurred after two weeks, while prior to this no subtype marker upregulation was present. In experiments with OPN, described in the literature, 3 days of treatment were sufficient to achieve a subtype shift 1. However, in these experiments, cell lines were used as the cancer model, making direct comparisons impossible. Nevertheless, this result indicates that secreted factors such as cytokines released by PDO42 induced a subtype shift in the classical organoid line PDO18. Furthermore, it highlights the role of tumor intrinsic secreted factors to maintain and induce the basal-like subtype in an autocrine role. In the literature secreted factors, by the tumor, are mostly associated to their role of shaping the TME <sup>29,98</sup>. One example would be the recruitment of tumor associated macrophages, which induces a basal-like subtype via secreted TNF-α

<sup>101</sup>. One highly expressed cytokine by PDO42 would be OPN, although the cytokine array showed the expression of other cytokines (which are however not directly associated with EMT) as well. To answer the question, if OPN was the responsible cytokine, a repetition of this experiment with additionally supernatant from a SPP1 KO organoid line could be performed.

## 4.5 The composition of the culture medium has an influence on the subtype markers

In the literature, the organoid cohort showed consisted subtype scores between early and late passages, although a slight tendency towards increased classical signatures was observed as well <sup>35</sup>. To further analyze how the culture medium composition affects the subtype, the basal-like PDO100 was cultured for 40 days in different culture mediums. This line was chosen, since the qPCR analysis showed a decreased SPP1 and basal-like subtype marker expression, compared to what would be expected from the RNA-seq. This suggested a high susceptibility for subtype changes in this organoid line. The experiment shows that the basal-like subtype marker expression and SPP1 expression decreases in all analyzed media. Interestingly, the medium with the least niche factors, Medium C (containing only EGF, FGF and RSPO-1) showed the most stable expression. The effect on the classical markers seemed to be less clearly defined. However, since only a few subtype markers were analyzed, it is difficult to reach to a definitive conclusion. The observed results provide evidence that the medium composition can affect the subtype, therefore it might be an interesting approach to find a special subtype stabilizing medium for basal-like PDAC organoids.

#### 4.6 Limitations

An important part of PDAC is the tumor microenvironment, which cannot be thoroughly analyzed with an organoid model alone. In particular, it has been described, that OPN can interact in the TME as well, further supporting the basal-like subtype <sup>3,51</sup>. These interactions with the TME could possibly be a part of the role of OPN in modulating the PDAC subtype. Therefore, further experiments using CAF coculture could bring further insights the into the OPN-TME interactions. Beside the lacking TME, organoids are still an in-vitro model. To ultimately confirm the effect of OPN on the PDAC subtype an in-vivo study would be necessary. An initial start could be the growth comparison of xenografts from SPP1 KO and WT organoids.

Beside the limitations of organoids as an in-vitro model, the high maintenance of organoids prohibited the analysis of multiple different organoid lines. Most experiments showed promising results; however due to the limited number, they should rather be considered as first indications.

To gain a better insight into the molecular mechanisms and the extent of an OPN-induced subtype shift further RNA-seq analysis should be performed. In this context the analysis of the SPP1 KO organoid cohort and a repeated rec. OPN treatment experiment could lead to further promising results.

#### 4.7 Conclusion

In conclusion this work confirms the subtype-modulating role of OPN in PDAC using a patient derived organoid model. In a basal-like organoid line, a CRISPR/cas9 mediated SPP1 KO led to an increase in the classical signature. A subsequent analysis regarding the chemotherapeutic sensitivity did not reveal any effect of an SPP1 KO. Additionally the treatment of classical organoids with rec. OPN lead to an upregulation of basal-like markers. Despite these findings, it is imperative to acknowledge the necessity of further research to understand the regulatory pathways OPN interacts with in PDAC. Additionally, the possible influence of OPN in the TME remains a critical aspect that could not be analyzed with organoids alone. Nevertheless, these results show that OPN can modulate the subtype identity in PDAC. Consequently the identification of OPN as a potential therapeutic target holds promise for the development of novel treatment options in PDAC.

# References

- 1. Adams, C. R. et al. Transcriptional control of subtype switching ensures adaptation and growth of pancreatic cancer. Elife 8, (2019).
- 2. Zhao, H. et al. The role of osteopontin in the progression of solid organ tumour. Cell Death and *Disease* vol. 9 Preprint at https://doi.org/10.1038/s41419-018-0391-6 (2018).
- 3. Kothari, A. N. et al. Osteopontin—a master regulator of epithelial-mesenchymal transition. Journal of Clinical Medicine vol. 5 Preprint at https://doi.org/10.3390/jcm5040039 (2016).
- 4. Drost, J. & Clevers, H. Organoids in cancer research. Nature Reviews Cancer vol. 18 407-418 Preprint at https://doi.org/10.1038/s41568-018-0007-6 (2018).
- 5. Ryan, D. P., Hong, T. S. & Bardeesy, N. Pancreatic Adenocarcinoma. New England Journal of Medicine **371**, 1039–1049 (2014).
- 6. Rahib, L. et al. Projecting cancer incidence and deaths to 2030: The unexpected burden of thyroid, liver, and pancreas cancers in the united states. Cancer Research vol. 74 2913–2921 Preprint at https://doi.org/10.1158/0008-5472.CAN-14-0155 (2014).
- 7. Siegel, R. L., Miller, K. D., Fuchs, H. E. & Jemal, A. Cancer statistics, 2022. CA Cancer J Clin 72, 7-33 (2022).
- 8. Strobel, O., Neoptolemos, J., Jäger, D. & Büchler, M. W. Optimizing the outcomes of pancreatic cancer surgery. Nature Reviews Clinical Oncology vol. 16 11-26 Preprint at https://doi.org/10.1038/s41571-018-0112-1 (2019).
- 9. Strobel, O. et al. Actual Five-year Survival After Upfront Resection for Pancreatic Ductal Adenocarcinoma. Ann Surg 275, 962–971 (2022).
- 10. Conroy, T. et al. FOLFIRINOX or Gemcitabine as Adjuvant Therapy for Pancreatic Cancer. New England Journal of Medicine **379**, 2395–2406 (2018).
- 11. Jones, S. et al. Core Signaling Pathways in Human Pancreatic Cancers Revealed by Global Genomic Analyses. www.sciencemag.orgSCIENCEVOL.
- 12. Raphael, B. J. et al. Integrated Genomic Characterization of Pancreatic Ductal Adenocarcinoma. Cancer Cell 32, 185-203.e13 (2017).
- 13. Morris, J. P., Wang, S. C. & Hebrok, M. KRAS, Hedgehog, Wnt and the twisted developmental biology of pancreatic ductal adenocarcinoma. Nature Reviews Cancer vol. 10 683-695 Preprint at https://doi.org/10.1038/nrc2899 (2010).
- 14. Collisson, E. A. et al. Subtypes of pancreatic ductal adenocarcinoma and their differing responses to therapy. *Nat Med* **17**, 500–503 (2011).
- 15. Moffitt, R. A. et al. Virtual microdissection identifies distinct tumor- and stroma-specific subtypes of pancreatic ductal adenocarcinoma. Nat Genet 47, 1168–1178 (2015).
- 16. Bailey, P. et al. Genomic analyses identify molecular subtypes of pancreatic cancer. Nature 531, 47-52 (2016).
- 17. Martinelli, P. et al. GATA6 regulates EMT and tumour dissemination, and is a marker of response to adjuvant chemotherapy in pancreatic cancer. Gut 66, 1665–1676 (2017).

- 18. Kloesch, B. et al. A GATA6-centred gene regulatory network involving HNFs and "np63 controls plasticity and immune escape in pancreatic cancer. Gut 71, 766–777 (2022).
- 19. Damrauer, J. S. et al. Intrinsic subtypes of high-grade bladder cancer reflect the hallmarks of breast cancer biology. Proc Natl Acad Sci U S A 111, 3110-3115 (2014).
- 20. Lomberk, G. et al. Distinct epigenetic landscapes underlie the pathobiology of pancreatic cancer subtypes. Nat Commun 9, (2018).
- 21. Krieger, T. G. et al. Single-cell analysis of patient-derived PDAC organoids reveals cell state heterogeneity and a conserved developmental hierarchy. Nat Commun 12, (2021).
- 22. Chan-Seng-Yue, M. et al. Transcription phenotypes of pancreatic cancer are driven by genomic events during tumor evolution. Nat Genet 52, 231-240 (2020).
- 23. Williams, H. L. et al. Spatially Resolved Single-Cell Assessment of Pancreatic Cancer Expression Subtypes Reveals Co-expressor Phenotypes and Extensive Intratumoral Heterogeneity. Cancer Res 83, 441-455 (2023).
- 24. Flowers, B. M. et al. Cell of origin influences pancreatic cancer subtype. Cancer Discov 11, 660-677 (2021).
- 25. Shinkawa, T. et al. Subtypes in pancreatic ductal adenocarcinoma based on niche factor dependency show distinct drug treatment responses. Journal of Experimental and Clinical Cancer Research 41, (2022).
- 26. Ho, W. J., Jaffee, E. M. & Zheng, L. The tumour microenvironment in pancreatic cancer — clinical challenges and opportunities. Nature Reviews Clinical Oncology vol. 17 527-540 Preprint at https://doi.org/10.1038/s41571-020-0363-5 (2020).
- 27. Feig, C. et al. The pancreas cancer microenvironment. Clinical Cancer Research vol. 18 4266-4276 Preprint at https://doi.org/10.1158/1078-0432.CCR-11-3114 (2012).
- 28. Rhim, A. D. et al. Stromal elements act to restrain, rather than support, pancreatic ductal adenocarcinoma. *Cancer Cell* **25**, 735–747 (2014).
- 29. Öhlund, D. et al. Distinct populations of inflammatory fibroblasts and myofibroblasts in pancreatic cancer. J Exp Med 214, 579-596 (2017).
- 30. Tod, J., Jenei, V., Thomas, G. & Fine, D. Tumor-stromal interactions in pancreatic cancer. Pancreatology vol. 13 1-7 Preprint at https://doi.org/10.1016/j.pan.2012.11.311 (2013).
- 31. Bulle, A. & Lim, K. H. Beyond just a tight fortress: contribution of stroma to epithelialmesenchymal transition in pancreatic cancer. Signal Transduction and Targeted Therapy vol. 5 Preprint at https://doi.org/10.1038/s41392-020-00341-1 (2020).
- 32. Özdemir, B. C. et al. Depletion of carcinoma-associated fibroblasts and fibrosis induces immunosuppression and accelerates pancreas cancer with reduced survival. Cancer Cell 25, 719-734 (2014).
- 33. Aung, K. L. et al. Genomics-driven precision medicine for advanced pancreatic cancer: Early results from the COMPASS trial. Clinical Cancer Research 24, 1344–1354 (2018).
- 34. Tiriac, H. et al. Organoid profiling identifies common responders to chemotherapy in pancreatic cancer. Cancer Discov 8, 1112-1129 (2018).



- 35. Le Blanc, S. et al. Deep molecular characterization linked to drug response profiling of pancreatic ductal adenocarcinoma using patient-derived organoids. bioRxiv (2021).
- 36. Porter, R. L. et al. Epithelial to mesenchymal plasticity and differential response to therapies in pancreatic ductal adenocarcinoma. doi:10.1073/pnas.1914915116/-/DCSupplemental.
- 37. Hwang, W. L. et al. Single-nucleus and spatial transcriptomics of archival pancreatic cancer multi-compartment reveals reprogramming after neoadjuvant treatment. doi:10.1101/2020.08.25.267336.
- 38. Singh, A. et al. A Gene Expression Signature Associated with 'K-Ras Addiction' Reveals Regulators of EMT and Tumor Cell Survival. Cancer Cell 15, 489–500 (2009).
- 39. Kijewska, M. et al. The embryonic type of SPP1 transcriptional regulation is re-activated in qlioblastoma. Oncotarget vol. 8 www.impactjournals.com/oncotarget/ (2017).
- 40. Oldberg, A., Franzfn, A. & Heinegard, D. Cloning and sequence analysis of rat bone sialoprotein (osteopontin) cDNA reveals an Arg-Gly-Asp cell-binding sequence (cell adhesion/bone matrix proteins/glycosylation). Biochemistry vol. 83 https://www.pnas.org (1986).
- Mckee, M. D. & Nanci, A. Osteopontin: An Interfacial Extracellular Matrix Protein in Mineralized 41. Tissues. Connect Tissue Res 35, 197–205 (1996).
- 42. Kim, J. M., Kim, M. Y., Lee, K. & Jeong, D. Distinctive and selective route of PI3K/PKCα-PKC\u03b8/RhoA-Rac1 signaling in osteoclastic cell migration. Mol Cell Endocrinol 437, 261-267 (2016).
- 43. Zou, C. et al. Osteopontin Promotes Mesenchymal Stem Cell Migration and Lessens Cell Stiffness via Integrin β1, FAK, and ERK Pathways. Cell Biochem Biophys 65, 455–462 (2013).
- 44. Oldberg, A., Franzfn, A. & Heinegard, D. Cloning and sequence analysis of rat bone sialoprotein (osteopontin) cDNA reveals an Arg-Gly-Asp cell-binding sequence (cell adhesion/bone matrix proteins/glycosylation). Biochemistry vol. 83 https://www.pnas.org (1986).
- 45. Li, C. et al. Identification of pancreatic cancer stem cells. Cancer Res 67, 1030–1037 (2007).
- 46. Si, J. et al. Osteopontin in Bone Metabolism and Bone Diseases. Medical Science Monitor vol. 26 Preprint at https://doi.org/10.12659/MSM.919159 (2020).
- 47. Kazanecki, C. C., Uzwiak, D. J. & Denhardt, D. T. Control of osteopontin signaling and function by post-translational phosphorylation and protein folding. Journal of Cellular Biochemistry vol. 102 912–924 Preprint at https://doi.org/10.1002/jcb.21558 (2007).
- 48. Inoue, M. & Shinohara, M. L. Intracellular osteopontin (iOPN) and immunity. Immunologic Research vol. 49 160–172 Preprint at https://doi.org/10.1007/s12026-010-8179-5 (2011).
- 49. Ogawa, D. et al. Liver x receptor agonists inhibit cytokine-induced osteopontin expression in macrophages through interference with activator protein-1 signaling pathways. Circ Res 96, (2005).
- 50. Hullinger, T. G., Pan, Q., Viswanathan, H. L. & Somerman, M. J. TGFβ and BMP-2 activation of the OPN promoter: Roles of Smad- and Hox-binding elements. Exp Cell Res 262, 69–74 (2001).
- 51. Castello, L. M. et al. Osteopontin at the Crossroads of Inflammation and Tumor Progression. Mediators of Inflammation vol. 2017 Preprint at https://doi.org/10.1155/2017/4049098 (2017).

- 52. Tang, Z., Kang, B., Li, C., Chen, T. & Zhang, Z. GEPIA2: an enhanced web server for large-scale expression profiling and interactive analysis. Nucleic Acids Res 47, W556-W560 (2019).
- 53. Rangaswami, H., Bulbule, A. & Kundu, G. C. Osteopontin: role in cell signaling and cancer progression. Trends Cell Biol 16, 79-87 (2006).
- 54. Steinman, L. A molecular trio in relapse and remission in multiple sclerosis. Nat Rev Immunol 9, 440-447 (2009).
- 55. Urtasun, R. et al. Osteopontin, an oxidant stress sensitive cytokine, up-regulates collagen-I via integrin  $\alpha$  V $\beta$  3 engagement and PI3K/pAkt/NF $\kappa$ B signaling. Hepatology **55**, 594–608 (2012).
- 56. Li, N. Y. et al. Osteopontin Up-Regulates Critical Epithelial-Mesenchymal Transition Transcription Factors to Induce an Aggressive Breast Cancer Phenotype. J Am Coll Surg 217, 17-26 (2013).
- 57. Kothari, A. N., Mi, Z., Zapf, M. & Kuo, P. C. Novel clinical therapeutics targeting the epithelial to mesenchymal transition. Clin Transl Med 3, (2014).
- 58. Guan, J. et al. Retinoic acid inhibits pancreatic cancer cell migration and EMT through the downregulation of IL-6 in cancer associated fibroblast cells. Cancer Lett 345, 132-139 (2014).
- 59. Weber. Categorical meta-analysis of Osteopontin as a clinical cancer marker. Oncol Rep 25, (2011).
- 60. Koopmann, J. et al. Evaluation of Osteopontin as Biomarker for Pancreatic Adenocarcinoma. Epidemiol Biomarkers *Prev* vol. 13 http://aacrjournals.org/cebp/articlepdf/13/3/487/1938691/487-491.pdf (2004).
- 61. Maeda, N. et al. Osteopontin-integrin interaction as a novel molecular target for antibodymediated immunotherapy in adult T-cell leukemia. Retrovirology 12, (2015).
- 62. Liu, Y. et al. Osteopontin Promotes Hepatic Progenitor Cell Expansion and Tumorigenicity via Activation of  $\beta$ -Catenin in Mice. Stem Cells **33**, 3569–3580 (2015).
- 63. Shojaei, F. et al. Osteopontin induces growth of metastatic tumors in a preclinical model of nonsmall lung cancer. Journal of Experimental and Clinical Cancer Research 31, (2012).
- 64. Farrokhi, V., Chabot, J. R., Neubert, H. & Yang, Z. Assessing the Feasibility of Neutralizing Osteopontin with Various Therapeutic Antibody Modalities. Sci Rep 8, (2018).
- 65. Boumans, M. J. H. et al. Safety, tolerability, pharmacokinetics, pharmacodynamics and efficacy of the monoclonal antibody ASK8007 blocking osteopontin in patients with rheumatoid arthritis: a randomised, placebo controlled, proof-of-concept study. Ann Rheum Dis 71, 180-185 (2012).
- 66. Tentler, J. J. et al. Patient-derived tumour xenografts as models for oncology drug development. Reviews Clinical Oncology vol. 338-350 Preprint at https://doi.org/10.1038/nrclinonc.2012.61 (2012).
- 67. Kamb, A. What's wrong with our cancer models? Nat Rev Drug Discov 4, 161-165 (2005).
- 68. Corrò, C., Novellasdemunt, L. & Li, V. W. A brief history of organoids. Am J Physiol Cell Physiol 319, 151-165 (2020).



- 69. Porter, R. J., Murray, G. I. & McLean, M. H. Current concepts in tumour-derived organoids. British Journal of Cancer vol. 123 1209-1218 Preprint at https://doi.org/10.1038/s41416-020-0993-5 (2020).
- 70. Boj, S. F. et al. Organoid models of human and mouse ductal pancreatic cancer. Cell 160, 324-338 (2015).
- 71. Hwang, C. II, Boj, S. F., Clevers, H. & Tuveson, D. A. Preclinical models of pancreatic ductal 238 197-204 Preprint adenocarcinoma. Journal of Pathology vol. https://doi.org/10.1002/path.4651 (2016).
- 72. Seino, T. et al. Human Pancreatic Tumor Organoids Reveal Loss of Stem Cell Niche Factor Dependence during Disease Progression. Cell Stem Cell 22, 454-467.e6 (2018).
- 73. Kleinman, H. K. & Martin, G. R. Matrigel: Basement membrane matrix with biological activity. Seminars in Cancer Biology vol. 15 378-386 **Preprint** https://doi.org/10.1016/j.semcancer.2005.05.004 (2005).
- 74. Hughes, C. S., Postovit, L. M. & Lajoie, G. A. Matrigel: a complex protein mixture required for optimal growth of cell culture. Proteomics 10, 1886–1890 (2010).
- 75. Conant, D. et al. Inference of CRISPR Edits from Sanger Trace Data. CRISPR J 5, 123–130 (2022).
- 76. Crowell, H. L. et al. On the discovery of subpopulation-specific state transitions from multisample multi-condition single-cell RNA sequencing data. doi:10.1101/713412.
- 77. Tarca, A. L. et al. A novel signaling pathway impact analysis. Bioinformatics 25, 75–82 (2009).
- 78. Luo, W. & Brouwer, C. Pathview: An R/Bioconductor package for pathway-based data integration and visualization. *Bioinformatics* **29**, 1830–1831 (2013).
- 79. Ulgen, E., Ozisik, O. & Sezerman, O. U. PathfindR: An R package for comprehensive identification of enriched pathways in omics data through active subnetworks. Front Genet 10, (2019).
- 80. Kolde, R. & Vilo, J. GOsummaries: An R Package for Visual Functional Annotation of Experimental Data. F1000Res 4, (2015).
- 81. Raghavan, S. et al. Microenvironment drives cell state, plasticity, and drug response in pancreatic cancer. Cell **184**, 6119-6137.e26 (2021).
- 82. Schindelin, J. et al. Fiji: An open-source platform for biological-image analysis. Nature Methods vol. 9 676–682 Preprint at https://doi.org/10.1038/nmeth.2019 (2012).
- 83. Ihry, R. J. et al. P53 inhibits CRISPR-Cas9 engineering in human pluripotent stem cells. Nat Med **24**, 939–946 (2018).
- 84. Gry, M. et al. Correlations between RNA and protein expression profiles in 23 human cell lines. BMC Genomics 10, (2009).
- 85. Roshani, R., McCarthy, F. & Hagemann, T. Inflammatory cytokines in human pancreatic cancer. Cancer Letters vol. 345 157-163 Preprint at https://doi.org/10.1016/j.canlet.2013.07.014 (2014).
- Doench, J. G. et al. Optimized sgRNA design to maximize activity and minimize off-target effects 86. of CRISPR-Cas9. Nat Biotechnol 34, 184-191 (2016).

- 87. Das, R., Philip, S., Mahabeleshwar, G. H., Bulbule, A. & Kundu, G. C. Osteopontin: It's role in regulation of cell motility and nuclear factor κB-mediated urokinase type plasminogen activator expression. **IUBMB** 441-447 Life vol. 57 **Preprint** https://doi.org/10.1080/15216540500159424 (2005).
- 88. Chen, Y.-J. et al. Osteopontin increases migration and MMP-9 up-regulation via  $\alpha v\beta 3$  integrin, FAK, ERK, and NF-kB-dependent pathway in human chondrosarcoma cells. J Cell Physiol 221, 98-108 (2009).
- 89. Hamacher-Brady, A. & Brady, N. R. Mitophagy programs: Mechanisms and physiological implications of mitochondrial targeting by autophagy. Cellular and Molecular Life Sciences vol. 73 775–795 Preprint at https://doi.org/10.1007/s00018-015-2087-8 (2016).
- 90. Liu, G. et al. Osteopontin induces autophagy to promote chemo-resistance in human hepatocellular carcinoma cells. Cancer Lett 383, 171–182 (2016).
- 91. Yang, M. C. et al. Blockade of autophagy reduces pancreatic cancer stem cell activity and potentiates the tumoricidal effect of gemcitabine. Mol Cancer 14, (2015).
- 92. Binns, D. et al. QuickGO: A web-based tool for Gene Ontology searching. Bioinformatics 25, 3045-3046 (2009).
- 93. Koh, A. et al. Role of osteopontin in neutrophil function. Immunology 122, 466–475 (2007).
- 94. Caunt, C. J. & Keyse, S. M. Dual-specificity MAP kinase phosphatases (MKPs): Shaping the outcome of MAP kinase signalling. FEBS Journal vol. 280 489-504 Preprint at https://doi.org/10.1111/j.1742-4658.2012.08716.x (2013).
- 95. Eberl, M. et al. Hedgehog-EGFR cooperation response genes determine the oncogenic phenotype of basal cell carcinoma and tumour-initiating pancreatic cancer cells. EMBO Mol Med 4, 218–233 (2012).
- 96. Khan, Z. E., Wang, T. C., Cui, G., Chi, A. L. & Dimaline, R. Transcriptional regulation of the human trefoil factor, TFF1, by gastrin. Gastroenterology 125, 510-521 (2003).
- 97. Lan, T., Chen, L. & Wei, X. Inflammatory cytokines in cancer: Comprehensive understanding and Cells vol. 10 1-16 clinical progress in gene therapy. Preprint at https://doi.org/10.3390/cells10010100 (2021).
- 98. Espinet, E., Klein, L., Puré, E. & Singh, S. K. Mechanisms of PDAC subtype heterogeneity and therapy response. **Trends** in Cancer vol. 1060-1071 Preprint https://doi.org/10.1016/j.trecan.2022.08.005 (2022).
- 99. Zheng, X. et al. Epithelial-to-mesenchymal transition is dispensable for metastasis but induces chemoresistance in pancreatic cancer. *Nature* **527**, 525–530 (2015).
- Liebhoff, A. M. et al. Pathogen detection in RNA-seq data with Pathonoia. BMC Bioinformatics 100. **24**, (2023).
- 101. Tu, M. et al. TNF-α-producing macrophages determine subtype identity and prognosis via AP1 enhancer reprogramming in pancreatic cancer. Nat Cancer 2, 1185-1203 (2021).